

STUDY OF CARRIER FREQUENCY OFFSET ESTIMATION IN MIMO AND MIMO OFDM SYSTEMS USING TRAINING SEQUENCES

A DISSERTATION

*Submitted in partial fulfillment of the
requirements for the award of the degree*

of

MASTER OF TECHNOLOGY

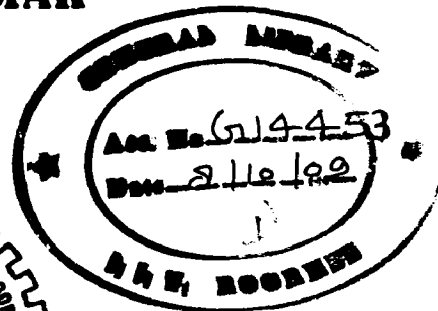
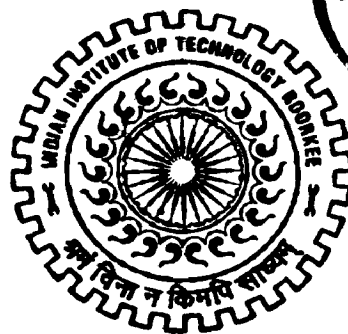
in

ELECTRONICS AND COMMUNICATION ENGINEERING

(With Specialization in Communication Systems)

By

T. VISHAL KUMAR



DEPARTMENT OF ELECTRONICS AND COMPUTER ENGINEERING
INDIAN INSTITUTE OF TECHNOLOGY ROORKEE
ROORKEE - 247 667 (INDIA)

JUNE, 2009

CANDIDATE'S DECLARATION

I hereby declare that the work, which is presented in this dissertation report entitled "***STUDY OF CARRIER FREQUENCY OFFSET ESTIMATION IN MIMO AND MIMO OFDM SYSTEMS USING TRAINING SEQUENCES***" towards the partial fulfillment of the requirements for the award of degree of *Master of Technology*, in *Electronics and Communication Engineering* with specialization in *Communication Systems*, submitted in the Department of Electronics and Computer Engineering, Indian Institute of Technology Roorkee, Roorkee (India) is an authentic record of my own work carried out during the period from July 2008 to June 2009, under the guidance of ***Dr. S. K. VARMA, Professor, Department of Electronics and Computer Engineering, Indian Institute of Technology Roorkee.***

I have not submitted the matter embodied in this dissertation for the award of any other Degree or Diploma.

Date: 29/06/09

Place: Roorkee



T. VISHAL KUMAR

CERTIFICATE

This is to certify that the above statement made by the candidate is correct to the best of my knowledge and belief.

Date: 29.6.09

Place: Roorkee


Dr. S. K. VARMA,
Professor, E&C E Department
IIT Roorkee,
Roorkee - 247 667 (India).

ACKNOWLEDGEMENTS

First of all, I would like to take this opportunity to extend my heartfelt gratitude to my guide and mentor ***Dr. S. K. VARMA***, Professor, Department of Electronics and Computer Engineering, Indian Institute of Technology Roorkee, who had offered me invaluable support, constructive guidance and helpful discussion throughout my dissertation work. I am grateful for his patience and kindness in answering my questions and revising my submitted reports. Without his continuous encouragement and stimulating suggestions I would have not completed my dissertation work.

I would like to thank all my classmates and my dearest friend ***Kshitiz Gupta*** for their valuable suggestions and comments which made this dissertation work much more clear. I would also like to thank lab assistants ***Mr. Mahendra Singh*** and ***Mr. Anand Krishna Yadav*** for their valuable support in completing my work. I want to thank all the people who help me throughout my study at IIT Roorkee.

Finally, I would like to thank my parents and family for their love, trust and encouragement throughout the two years. Without their support, it would have been impossible for me to accomplish what I have accomplished.

T.VISHAL KUMAR

LIST OF ABBREVIATIONS

Additive White Gaussian Noise.....	AWGN
Bit Error Rate.....	BER
Carrier Frequency Offset.....	CFO
Cyclic Prefix.....	CP
Cramer-Rao Lower Bound.....	CRLB
Cramer-Rao Bound.....	CRB
Chu sequence Based Training Sequence.....	CBTS
Digital Subscriber Line.....	DSL
Discrete Fourier Transform.....	DFT
Digital Audio Broadcasting.....	DAB
Digital Video Broadcasting.....	DVB
Enhanced Data Rates for GSM Evolution.....	EDGE
Enhanced Circuit Switched Data.....	ECSD
Enhanced General Packet Radio Service.....	EGPRS
Frequency Division Multiplexing.....	FDM
Forward Error Correction.....	FEC
Fast Fourier Transform.....	FFT
Fisher Information Matrix.....	FIM
Fractional Carrier Frequency Offset.....	FCFO
Global System for Mobile communications.....	GSM
General Packet Radio Service.....	GPRS
High- Speed Circuit Switched Data.....	HSCSD
Inter- Symbol Interference.....	ISI

Inverse Discrete Fourier Transform.....	IDFT
Inverse Fast Fourier Transform.....	IFFT
Inter Carrier Interference.....	ICI
Integer Carrier Frequency Offset.....	ICFO
Log Likelihood Function.....	LLF
Multiple-Input Multiple-Output.....	MIMO
Multiple Antenna Interference.....	MAI
Medium Access Control.....	MAC
Maximum Likelihood.....	ML
Mean Square Error.....	MSE
Minimum Variance Unbiased.....	MVU
Orthogonal Frequency Division Multiplexing.....	OFDM
Orthogonal Frequency Division Multiple Access.....	OFDMA
Physical Layer.....	PHY
Single-Input Single-Output.....	SISO
Signal to Noise Ratio.....	SNR
Universal Mobile Telephone System.....	UMTS
Wideband Code Division Multiple Access.....	WCDMA
Wireless Local Area Network.....	WLAN

LIST OF FIGURES

<i>Page No</i>	<i>Figure</i>	<i>Figure Caption</i>
4	Fig.1.1	Basic concept of OFDM system
5	Fig.1.2	Basic steps in OFDM technique
7	Fig1.3	The simplified block diagram of ($N_T \times N_R$) MIMO OFDM system
12	Fig.2.1	A basic block diagram of OFDM system
14	Fig.2.2 (a)	OFDM signal spectrum (3 carriers) without CFO
14	Fig.2.2 (b)	OFDM signal spectrum (3 carriers) with CFO
23	Fig.2.3	Comparision of SNR values at the output of DFT for the OFDM subcarriers effected by different values of relative frequency offset with their Theoretical lower bounds
25	Fig.2.4	Relative frequency offset estimated using Moose method Vs Actual relative frequency offset for $E_b/N_0 = 5$ and 17 dB.
28	Fig. 3.1	$N_T \times N_R$ MIMO system model
41	Fig.3.2	Comparison of Exact CRB and Asymptotic CRB for different training sequence lengths
43	Fig.3.3	Comparison of MSE performance of MLE method and Reduced complexity MLE method simulated for 4 x 1 MIMO system (using pseudo random sequence as training sequence and when channel is known)
44	Fig.3.4	Comparison of MSE performance of MLE method and Reduced complexity MLE method simulated for 4 x 2 MIMO system (using pseudo random sequence as training sequence and when channel is known)

<u>Page No</u>	<u>Figure</u>	<u>Figure Caption</u>
45	Fig.3.5	Comparison of MSE performance of MLE method and Reduced complexity MLE method simulated for 4 x 1 and 4 x 2 MIMO system (using pseudo random sequence as training sequence and when channel is known)
47	Fig.3.6	Comparison of MSE performance of MLE method and Reduced complexity MLE method simulated for 4 x 1 MIMO system (using pseudo random sequence as training sequence and when channel is Unknown)
48	Fig.3.7	Comparison of MSE performance of MLE method and Reduced complexity MLE method simulated for 4 x 2 MIMO system (using pseudo random sequence as training sequence and when channel is Unknown)
49	Fig.3.8	Comparison of MSE performance of MLE method and Reduced complexity MLE method simulated for 4 x 1 and 4 x 2 MIMO system (using pseudo random sequence as training sequence and when channel is Unknown)
51	Fig.3.9	Comparison of MSE performance of MLE method and Reduced complexity MLE method simulated for 4 x 1 MIMO system (using Orthogonal sequence as training sequence and when channel is Unknown)
52	Fig.3.10	Comparison of MSE performance of MLE method and Reduced complexity MLE method simulated for 4 x 2 MIMO system (using Orthogonal sequence as training sequence and when channel is Unknown)
53	Fig.3.11	Comparison of MSE performance of MLE method and Reduced complexity MLE method simulated for 4 x 1 and 4 x 2 MIMO system (using Orthogonal sequence as training sequence and when channel is Unknown)

<u>Page No</u>	<u>Figure</u>	<u>Figure Caption</u>
54	Fig.3.12	Comparison of MSE performance of Reduced complexity MLE method simulated for 4 x 1 and 4 x 2 MIMO system (using both pseudo random sequence and Orthogonal sequence as training sequences and when channel is Unknown)
57	Fig.4.1 (a)	Real part of Chu sequence $\{s_k\}$ of length $N=64$ and $M=21$
57	Fig.4.1 (b)	Imaginary part of Chu sequence $\{s_k\}$ of length $N=64$ & $M=21$
57	Fig.4.2	Autocorrelation values $\{x_j\}$ of Chu sequence of length $N=64$ and $M = 21$
59	Fig.4.3 (a)	Block diagram of $N_T \times N_R$ MIMO OFDM System Transmitter
59	Fig.4.3 (b)	Block diagram of $N_T \times N_R$ MIMO OFDM System Receiver
69	Fig.4.4	MSE performance of 3 x 2 MIMO OFDM system using different training sequences for CFO estimation
71	Fig.4.5	MSE performance of 3 x 2 MIMO OFDM system with simplified estimator using different training sequences
72	Fig.4.6	MSE performance of 3 X 2 MIMO OFDM system using different estimators using Chu sequence based training sequences (CBTS)

TABLE OF CONTENTS

CANDIDATE'S DECLARATION	i
ACKNOWLEDGEMENTS	ii
ABSTRACT	iii
LIST OF ABBREVIATIONS	iv
LIST OF FIGURES	vi
1. INTRODUCTION	
1.1. Motivation.....	1
1.2. Orthogonal Frequency Division Multiplexing (OFDM).....	3
1.3. Multiple-Input Multiple-Output (MIMO) Systems	5
1.4. MIMO OFDM Systems.....	6
1.5. Statement of Problem.....	8
1.6. Organization of Report.....	8
2. CARRIER FREQUENCY OFFSET ESTIMATION IN OFDM SYSTEMS	
2.1. Introduction.....	10
2.2. Effect of CFO on OFDM System Performance.....	11
2.3. Moose Method.....	18
2.4. Simulation Results.....	22
2.4.1. Results for Performance of OFDM System with and without CFO.....	22
2.4.2. Simulation Results of Moose Method.....	24
3. CARRIER FREQUENCY ESTIMATION METHOD IN MIMO SYSTEMS	
3.1. Introduction.....	26
3.2. System Model.....	27
3.3. CFO Estimation with Known Channel.....	29
3.3.1. ML Estimation.....	29
3.3.2. Computationally Efficient Estimation Method.....	30

3.4. CFO Estimation with Unknown Channel.....	31
3.4.1. Joint ML Estimation of Channel and CFO.....	31
3.4.2. Computationally Efficient Estimation Method.....	32
3.4.3. Training Sequence Design.....	34
3.5. Cramer-Rao Lower Bound.....	35
3.6. Simulation Results.....	40
3.6.1. Simulation Results of Exact CRB and Asymptotic CRB.....	40
3.6.2. Simulation Results of CFO Estimation with Known Channel (Using Pseudo Random Sequence as Training Sequence).....	42
3.6.3. Simulation Results of CFO Estimation with Unknown Channel (Using Pseudo Random Sequence as Training Sequence).....	46
3.6.4. Simulation Results of CFO Estimation with Unknown Channel (Using Orthogonal Sequence as Training Sequence).....	50
4. CARRIER FREQUENCY ESTIMATION METHODS IN MIMO OFDM SYSTEMS	
4.1. Introduction.....	55
4.2. Chu Sequences.....	56
4.3. System Model.....	58
4.4. CFO Estimation using Chu Sequence based Training Sequences (CBTS).....	60
4.5. Simplified CFO Estimation using Chu Sequence based Training Sequences (CBTS)	64
4.6. Simulation Results.....	68
4.6.1. Simulation Results of method discussed in section 4.4.....	68
4.6.2. Simulation Results of method discussed in section 4.5.....	70
5. CONCLUSIONS.....	73
6. REFERENCES.....	75

Chapter-1

Introduction

1.1 Motivation

Over the last two decade or so, we have witnessed a drastic increase in the demand for providing reliable high speed wireless communication links to support applications such as voice, video, e-mail, web browsing, to name a few. This is a challenging task, however, since transmission through a wireless link is prone to a number of impairments of which the most important are fading and interference. In addition, in wideband communications (i.e., at high data rates), the signal bandwidth is normally larger than the channel bandwidth and this gives rise to frequency selective fading which occurs due to multipath components.

If we look at the evolution of wireless communication, it is among one of the biggest success stories of last two decades not only from a scientific point of view, where the progress has been phenomenal, but also in terms of market size and impact on society. In fact wireless communication permeates in every aspect of our lives. As the demand for such high data rate applications is increasing, demand for bandwidth and spectral availability are endless as the wireless systems continue to strive for ever higher data rates. Multiple access wireless communication is being deployed for both fixed and mobile applications. In fixed applications, the wireless networks provide voice or data for fixed subscribers. Mobile networks offering voice and data services can be divided in to two classes: high mobility, to serve high speed vehicle borne users, and low mobility, to serve pedestrian users.

The gradual evolution of wireless communication systems follows the quest for high data rates, measured in bits/sec (bps) and with a high spectral efficiency, measured in bps/Hz. The first mobile communication systems were analog and are today referred to as systems of the first generation (1G). In the beginning of 1990s, the first digital systems emerged, denoted as second generation (2G) systems, the most popular 2G system introduced was the Global System for Mobile communications (GSM), which operates in the 900MHz or the

1800MHz band and supports data rates up to 22.8 Kbps. To accomplish higher data rates, two add-ons were developed for GSM, namely High-Speed Circuit Switched Data (HSCSD) and the General Packet Radio Service (GPRS), providing data rates up to 38.4 Kbps and 172.2 Kbps, respectively [1].

The demand for yet higher data rates forced the development of a new generation of wireless systems, the so called third generation (3G). These systems are characterized by a maximum data rate of at least 384 Kbps for mobile and 2 Mbps for indoors.

One of the leading technologies for 3G systems is the well known Universal Mobile Telephone System (UMTS) [also referred to as Wideband Code Division Multiple Access (WCDMA)]. UMTS represents a revolution in terms of services and data speeds from today's 2G's mobile networks. UMTS and WCDMA are already a reality and have been used in many parts of the world. To yield 3G data rates, an alternative approach was made with the Enhanced Data Rates for GSM Evolution (EDGE) concept. The EDGE system is based on GSM and operates in the same frequency bands. The significantly enhanced data rates are obtained by means of a new modulation scheme, which is more efficient than the GSM modulation scheme. As for GSM, two add-ons were developed for EDGE, namely Enhanced Circuit Switched Data (ECSD) and the Enhanced General Packet Radio Service (EGPRS). The maximum data rate of the EDGE system is 473.6 Kbps, which is accomplished by means of EGPRS. 2.5G systems, based on GPRS technology, a natural evolutionary stepping stone towards UMTS also provided faster data services [2].

The goal of the next generation of wireless systems, i.e. fourth generation (4G) is to provide data rates yet higher than the ones of 3G while granting the same degree of user mobility. 4G is expected to deliver more advanced versions of the same improvements provided by 3G, such as enhanced multimedia, smooth streaming video, universal access and portability across all types of devices. 4G enhancements are expected to include world wide "roaming" capability. As was projected for the ultimate 3G system, 4G might actually connect the entire globe and be operable from any location on or above the surface of earth. This aspect makes it distinctly different from the technologies developed until now. One of the most popular and powerful 4G technique is *Orthogonal Frequency Division Multiplexing* (OFDM).

1.2 Orthogonal Frequency Division Multiplexing (OFDM)

Orthogonal frequency division multiplexing (OFDM) is one of the most favorable technologies deployed in 4G systems as it essentially transforms the frequency selective fading channel into a flat fading channel. Even though this technology has been discovered for more than forty years [3], its wide spread success in commercial applications started in 1990's with the introduction of Digital Subscriber Line (DSL) [4] which brought affordable broadband internet access to home users. OFDM was also adopted in the wireless local area network (WLAN) standards, such as IEEE 802.11a [5], IEEE802.11g [6] and the upcoming IEEE802.11n [7]. OFDM is also a potential candidate for the fourth generation mobile communication systems as it forms its physical layer standard [8].

OFDM has many advantages that satisfy our increasing demand in high bandwidth wireless communications.

- It is highly spectral efficient as it allows overlapping of subcarriers spectrum and as it divides the single frequency selective channel into number of parallel narrowband flat fading sub-channels it is highly immune to fading in wireless environment.
- It also eliminates inter-symbol interference (ISI) through the use of cyclic prefix technique.
- OFDM is computationally efficient by using FFT techniques to implement the modulation and demodulation functions. Meanwhile, as the cost of digital signal processor is dropping, OFDM systems become more affordable and easier to be implemented. OFDM is also a very flexible technology.
- It is not limited to simple single-input single-output (SISO) systems; it can be extended to multiple-input multiple-output (MIMO) systems for spatial diversity, or it can assign subsets of subcarriers to individual users for multiple access. Orthogonal Frequency Division Multiple Access (OFDMA) is one of the typical multiple access schemes derived from OFDM.

OFDM is a multicarrier transmission technique, which divides the single wideband channel into number of parallel narrowband channels called sub-channels; each subcarrier in each sub-channel is being modulated by a low rate data stream. We know that in frequency

division multiplexing (FDM) technique, lot of spectrum is wasted in the form of guard bands between the adjacent channels for channel isolation and filtering purposes. In a typical system, up to 50% of the total spectrum is wasted in this manner. This problem becomes worse as the sub-channel bandwidth becomes narrower and total frequency band increases.

But, as mentioned earlier OFDM technique over comes this problem by splitting the available bandwidth into number of parallel narrowband sub-channels. The subcarriers of each sub-channel are made orthogonal to one another, allowing them to be spaced very close together with no overhead (like guard bands), as in FDM. This basic concept of OFDM saving the spectrum is illustrated in Fig.1.1.

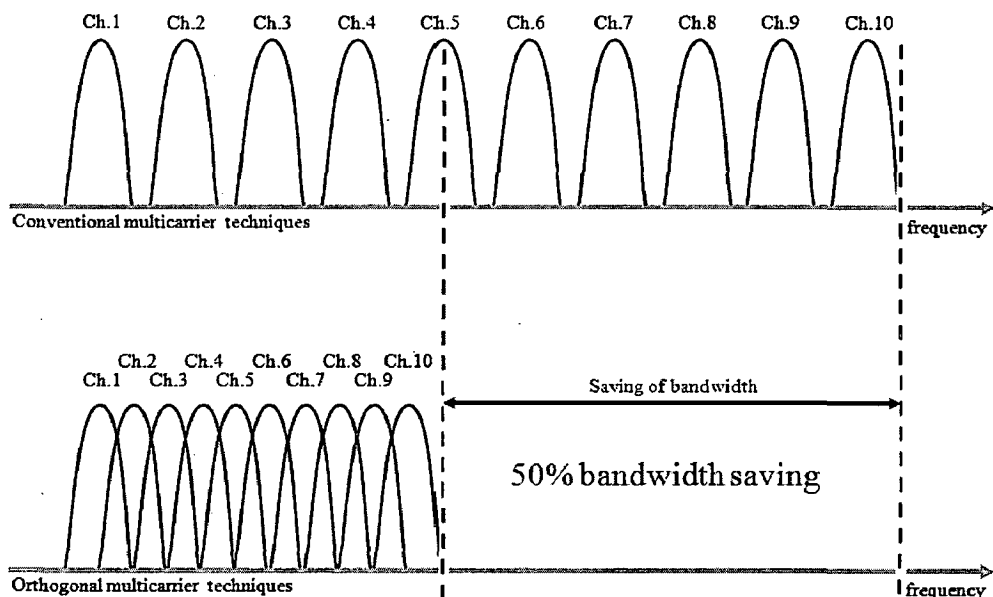


Fig.1.1 Basic concept of OFDM system

The basic steps performed in the OFDM system are shown in Fig.1.2. To generate OFDM signal, the high data rate input stream is converted into number of low data rate stream using serial to parallel converter. Each subcarrier is modulated with one of this low data rate streams in IFFT block and finally this signal is transmitted serially after adding cyclic prefix. At the receiver, exactly opposite steps are carried out as shown in Fig.1.2. Since each parallel sub-channel is essentially low data rate channel and since it is narrowband, it experiences flat fading. This is another advantage of OFDM technique, which will reduce the complexity of equalizer at the receiver end.

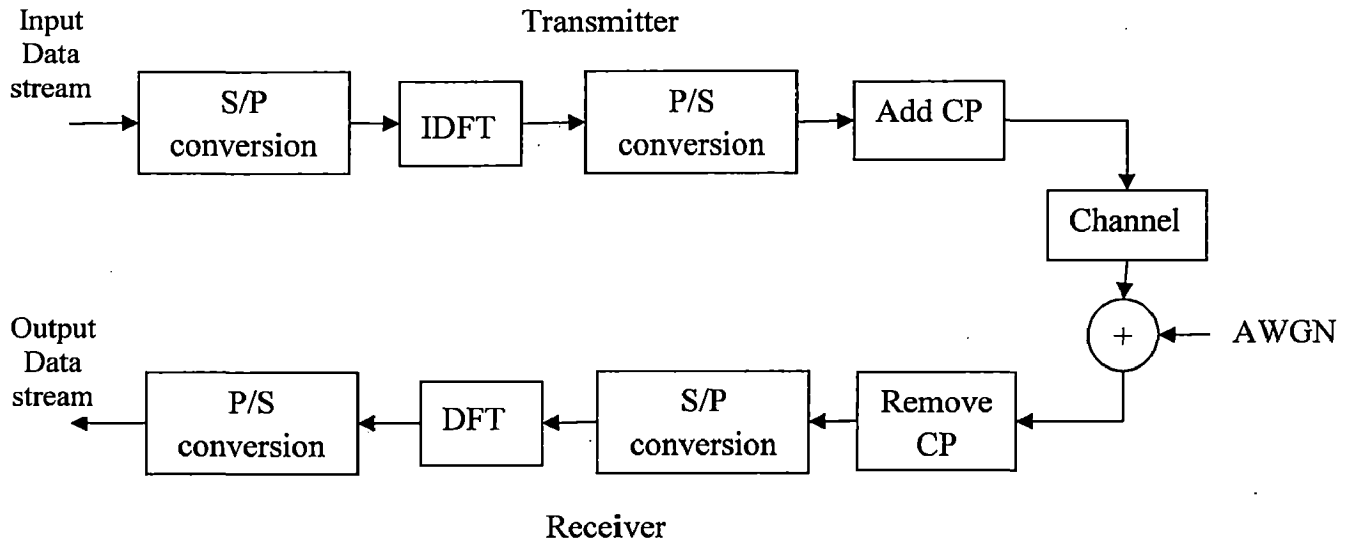


Fig.1.2 Basic steps in OFDM technique

1.3 Multiple-Input Multiple-Output (MIMO) Systems

Perhaps another one of the most interesting trends in wireless communication is the proposed use of multiple input multiple output systems. A MIMO system uses multiple transmitter antennas and multiple receiver antennas to break a multipath channel into several individual spatial channels. Now MIMO systems represent a huge change in how wireless communication systems are designed. This change reflects how we view multipath in a wireless system.

The Prospects of MIMO

From an information theoretic perspective, increasing the number of antennas essentially allows to achieve higher spectral efficiency compared to single-input single-output systems. Actual transmission schemes exploit this higher capacity by leveraging three types of partially contradictory gains:

- *Array gain* refers to picking up a larger share of the transmitted power at the receiver which mainly allows to extend the range of a communication system and to suppress interference.
- *Diversity gain* counters the effects of variations in the channel, known as fading, which increases link-reliability and QoS.

- *Multiplexing gain* allows for a linear increase in spectral efficiency and peak data rates by transmitting multiple data streams concurrently in the same frequency band. The number of parallel streams is thereby limited by the number of transmit or receive antennas, whichever is smaller.

Old Perspective: The ultimate goal of wireless communications is to combat the distortion caused by multipath in order to approach the theoretical limit of capacity for a band-limited channel.

New Perspective: Since multipath propagation actually represents multipath channels between a transmitter and receiver, the ultimate goal of wireless communications is to use multipath to provide higher total capacity than the theoretical limit for a conventional band limited channel.

The basic idea is to usefully exploit the multipath rather than mitigate it, considering the multipath itself as a source of diversity that allows the parallel transmission of independent data substreams from the same user. The exploitation of diversity and parallel transmission of several data streams on different propagation paths at the same time and frequency allows for extremely large capacities compared to conventional wireless systems. The prospect of many orders of magnitude improvement in wireless communication performance at no cost of extra spectrum (only hardware and complexity are added) is largely responsible for the success of MIMO.

1.4 MIMO OFDM Systems

For high data rate transmission, the multi-path characteristic of the environment causes the MIMO channel to be frequency selective. OFDM can transform such a frequency-selective MIMO channel into a set of parallel frequency flat MIMO channels, and therefore decrease receiver complexity. The combination of the two powerful techniques, MIMO and OFDM, is very attractive, and has become a most promising broadband wireless access scheme.

Fig.1.3 shows the simplified block diagram of $N_T \times N_R$ MIMO OFDM system. The source bit stream from data source is encoded by a forward error correction (FEC) encoder/

channel encoder. After that, the coded bit stream is mapped to a constellation by the digital modulator, and encoded by a MIMO encoder. Then each of the parallel output symbol streams corresponding to a certain transmit antenna follows the same transmission process. Firstly, these symbols are arranged in blocks and modulated by Inverse Discrete Fourier Transform (IDFT) or preferably Inverse Fast Fourier Transform (IFFT) to an OFDM symbol sequence. A cyclic prefix is attached to every OFDM symbol to mitigate the effect of channel delay spread, and a preamble is inserted in every slot for timing. Finally, the constructed data frame is transferred to IF/RF components for transmission.

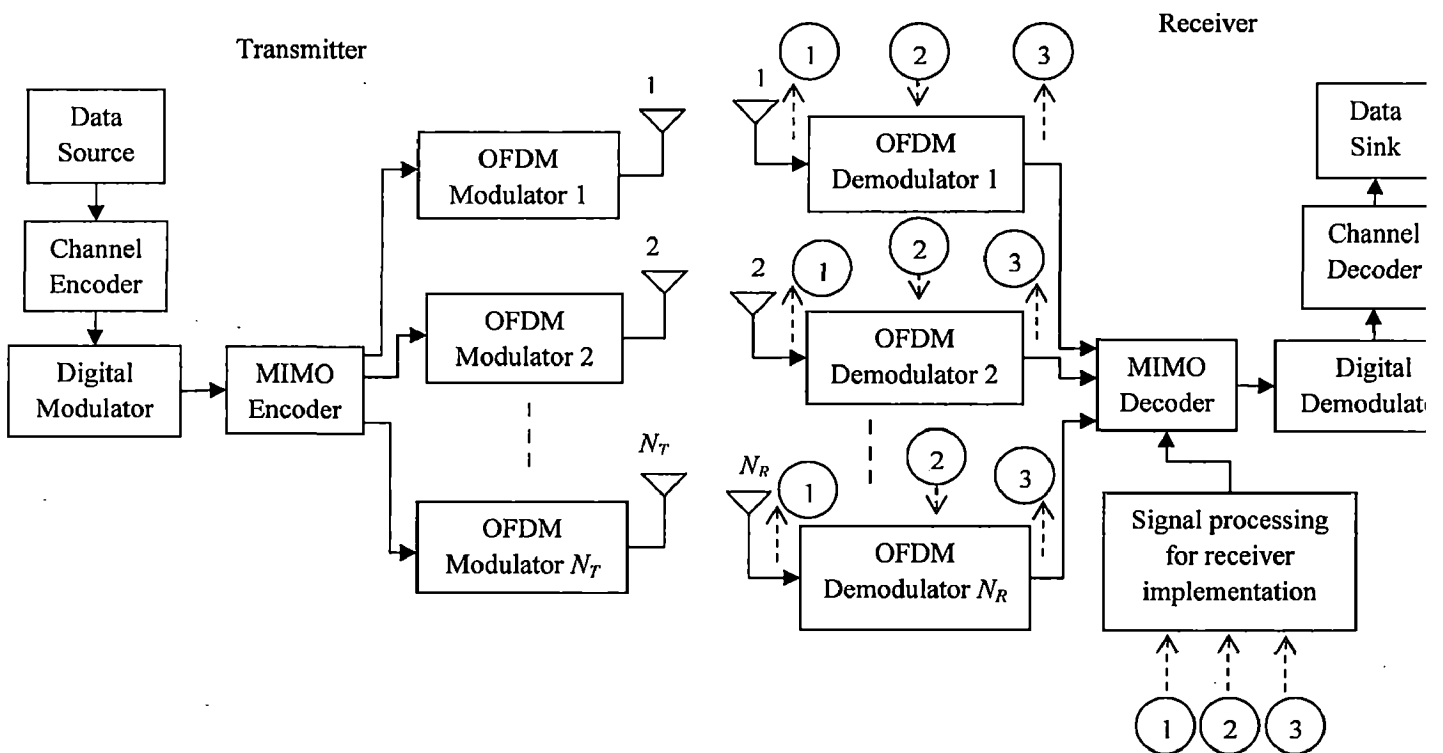


Fig.1.3 The simplified block diagram of $(N_T \times N_R)$ MIMO OFDM system

At the receiver end, received symbol stream from IF/RF components over the receive antennas are sent to OFDM demodulator, in which cyclic prefix is removed from the received symbol stream. Remaining OFDM symbol is demodulated by Discrete Fourier Transform (DFT) or Fast Fourier Transform (FFT). The output symbols of each OFDM demodulator are given to MIMO decoder to combine it into single high data rate stream. These symbols are de-mapped using digital demodulator and given to sink by performing channel decoding. There is a signal processing block for receiver implementation; this block

forms a main part of the receiver. Frequency and timing synchronization and channel estimation parts are carried on received symbols and the calculated parameters are used to in estimating the received symbols correctly.

As every system has its pros and cons, OFDM also suffers from its disadvantages. One of the major disadvantages is its extreme sensitivity to carrier frequency offset (CFO). Failing to synchronize the carrier frequency will destroy the orthogonality between subcarriers [9] and cause inter-carrier interference (ICI). So, accurate estimation and compensation of CFO is very important. Therefore, many synchronization schemes have been proposed for SISO OFDM systems. Some schemes are pilot based and some are based on blind estimation. Similar to SISO OFDM systems, MIMO OFDM systems are also sensitive to CFO, moreover for MIMO OFDM, there exists multi-antenna interference (MAI) between the received signals from different transmit antennas. The MAI makes CFO estimation more difficult, and a careful training sequence design is required for training-based CFO estimation in case of MIMO systems.

1.5 Statement of Problem

This work is aimed at performance study of carrier frequency offset estimators in MIMO and MIMO OFDM systems using training sequences.

The dissertation presents the following work

- Effect of CFO on the performance of SISO OFDM system
- CFO estimation techniques for MIMO systems using different training sequences and their performance analysis.
- CFO estimation techniques for MIMO OFDM systems using Chu sequence based training sequences.

1.6 Organization of Report

Chapter 1 gives brief introduction to the evolution of wireless systems through 2G, 3G and 4G systems. Following that, we will discuss about OFDM, MIMO and MIMO systems. Finally, it summarizes the statement of problem for the thesis work.

In Chapter 2 we discuss about the effect of CFO on the performance of the OFDM system. And discuss the Moose method which is one of the earliest CFO estimation techniques for OFDM system.

Chapter 3 starts with the discussion on CFO estimation for MIMO systems using training sequences. Firstly, we will discuss the ML estimation method and computationally efficient estimation method for two cases; known channel and unknown channel. Following that to overcome the drawbacks of computationally efficient estimation method when channel is unknown, we look at the training sequence design.

Chapter 4 discusses CFO estimation technique for MIMO OFDM systems which use Chu sequence based training sequences for the estimation purpose. We also discuss computationally efficient method which avoids complex polynomial rooting operation present in the earlier mentioned Chu sequence based estimation method.

Chapter 5 gives the conclusion of this thesis work.

Chapter-2

Carrier Frequency Offset Estimation in OFDM Systems

2.1 Introduction

Carrier frequency offset estimation can be performed in either time domain or frequency domain. In time domain CFO estimation methods, estimation is performed by sending known symbols after Inverse Discrete Fourier Transform block at transmitter and processing the received symbols before Discrete Fourier Transform block at the receiver, while in frequency domain CFO estimation methods, estimation is performed by sending known symbols before IDFT block at transmitter and processing the received symbols after DFT block at receiver [10]. Meanwhile, typical estimation methods can also be classified as:

1. Pilot or Training symbol aided [11], [12]
2. Cyclic prefix(CP) aided [13], [14]
3. Blind approach which utilizes the OFDM intrinsic structure information [15], [16]

Among them, CP aided methods in time domain are not so accurate, as the data within the guard interval is destroyed by ISI if the channel is heavily faded, while blind approach relies on signal statistics and often has high computational complexity, some blind approaches may have extra requirement of channel statistics too. Most CFO estimators rely on periodically transmitted pilots. However, pilot assisted methods are less attractive for continuous transmission OFDM based systems, such as Digital audio broadcasting (DAB) and Digital video broadcasting (DVB). Along with the potential benefit of improving spectral efficiency, this motivates blind CFO estimation in commercial systems. Furthermore, in non-cooperative (e.g., tactical) links, blind estimators are the only option, since training based ones cannot even be implemented [16].

In this section, we will consider brief overview of carrier frequency offset estimation techniques for SISO OFDM systems. Firstly, we will look at the effect of carrier frequency

offset on the performance of SISO OFDM system and thereafter we will mainly focus on training sequence based Moose's method [17]. We will cover CFO estimation techniques using training sequences for MIMO and MIMO OFDM systems in subsequent chapters.

2.2 Effect of CFO on OFDM System Performance

The typical block diagram of OFDM system is produced here for convenience in Fig.2.1. The data generated by the source is firstly passed to channel encoder to make the data more suitable for transmission by adding redundant bits. This data is then modulated using one of the well known modulation techniques such as QAM, QPSK. Let the n^{th} complex modulated symbol in baseband be denoted by d_n . After serial to parallel processing, these symbols are arranged into blocks. These blocks are then translated by IDFT or preferably Inverse Fast Fourier Transform, put them back into a symbol sequence or OFDM symbols by parallel to serial processing and transmitted serially [17].

In the other words, each symbol, d_n in the block represents the magnitude and phase of a virtual subcarrier in the frequency domain. The OFDM symbol can be expressed as

$$x_k = \frac{1}{N} \sum_{n=0}^{N-1} d_n e^{j \frac{2\pi}{N} nk} \quad k = 0, 1, 2, \dots, N-1 \quad (2.1)$$

where d_n are the complex modulated data symbols in baseband and N is the size of IFFT.

To avoid inter-symbol interference due to multipath effect, we insert cyclic prefix, a replica of the last several symbols of the block, in the beginning of the serial sequence after the parallel to serial conversion. This compensates the lost data due to multipath effect and simplifies the equalization at the receiver.

At the receiver, after removing CP, the OFDM symbols received, r_k are in the following form

$$r_k = \frac{1}{N} \sum_{n=0}^{N-1} h_n d_n e^{j \frac{2\pi}{N} nk} e^{j\theta} e^{j \frac{2\pi}{N} k \Delta f T} + w_k \quad k = 0, 1, 2, \dots, N-1 \quad (2.2)$$

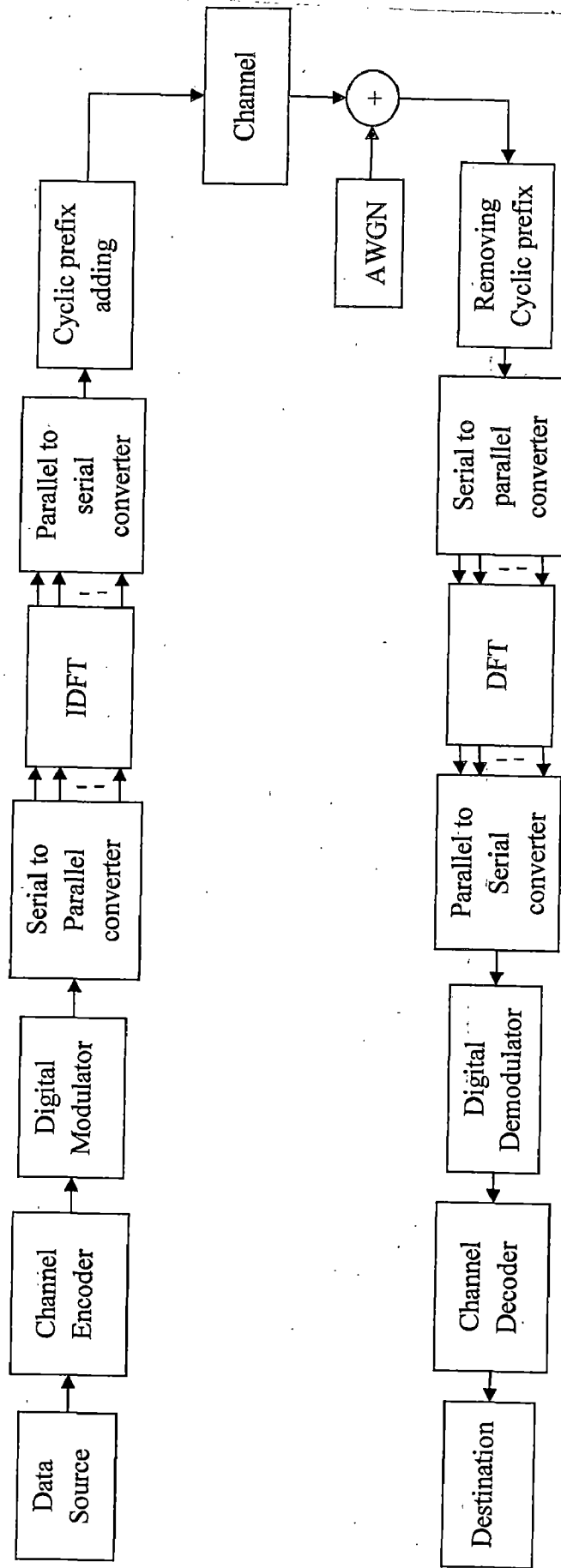


Fig.2.1 A basic block diagram of OFDM system

where h_n is the channel transfer function at subcarrier index n ,

θ is the carrier phase offset,

Δf is the carrier frequency offset,

T is the OFDM symbol period and

w_k are additive white Gaussian noise (AWGN).

The data sequence, y_m is recovered by applying DFT or preferably Fast Fourier Transform to the received OFDM symbols, r_k . Here, Eq.(2.3) shows the recovery of the m^{th} data symbol.

$$y_m = \sum_{k=0}^{N-1} r_k e^{-j\frac{2\pi mk}{N}} \quad m = 0, 1, 2, \dots, N-1 \quad (2.3)$$

To find the influence of the CFO to the recovered data symbols, we substitute Eq.(2.2) into Eq.(2.3). Then we have

$$y_m = \sum_{k=0}^{N-1} \left[\frac{1}{N} \sum_{n=0}^{N-1} h_n d_n e^{j\frac{2\pi}{N}nk} e^{j\theta} e^{j\frac{2\pi}{N}k\Delta f T} + w_k \right] e^{-j\frac{2\pi mk}{N}} \quad (2.4)$$

$$= \frac{1}{N} \sum_{k=0}^{N-1} \sum_{n=0}^{N-1} h_n d_n e^{j\frac{2\pi}{N}nk} e^{j\theta} e^{j\frac{2\pi}{N}k\Delta f T} e^{-j\frac{2\pi mk}{N}} + \sum_{k=0}^{N-1} w_k e^{-j\frac{2\pi mk}{N}}$$

Suppose $h_n = \delta_n$ for AWGN channel and neglect noise w_k for simplicity. We can simplify the above expression as

$$y_m = \frac{1}{N} \sum_{k=0}^{N-1} \sum_{n=0}^{N-1} d_n e^{j\frac{2\pi}{N}nk} e^{j\theta} e^{j\frac{2\pi}{N}k\Delta f T} e^{-j\frac{2\pi mk}{N}} \quad (2.5)$$

$$= \frac{1}{N} \sum_{k=0}^{N-1} \sum_{n=0}^{N-1} d_n e^{j\theta} e^{j\frac{2\pi}{N}k(n-m+\Delta f T)}$$

$$= \frac{1}{N} \sum_{n=0}^{N-1} d_n e^{j\theta} \cdot \left[\sum_{k=0}^{N-1} e^{j\frac{2\pi}{N}k(n-m+\Delta f T)} \right]$$

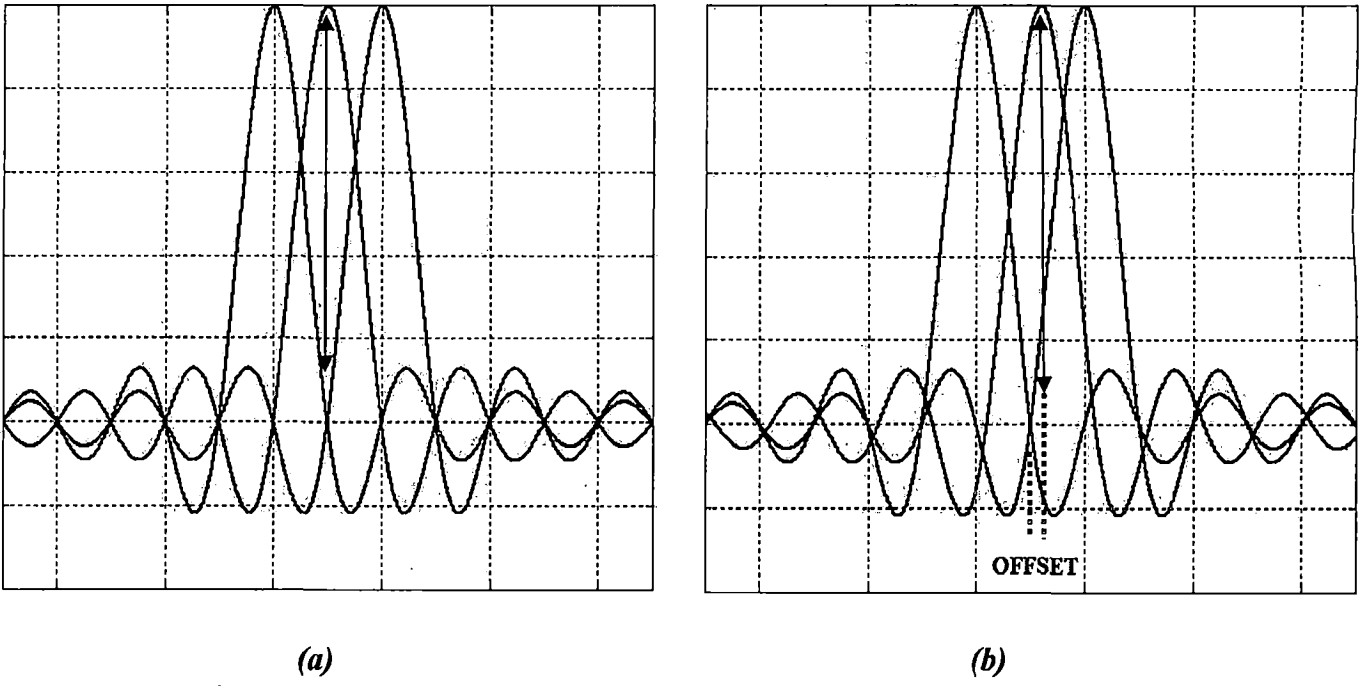


Fig.2.2 OFDM signal spectrum (3 carriers) (a) without CFO and (b) with CFO

$$\begin{aligned}
 &= \frac{1}{N} \sum_{n=0}^{N-1} d_n e^{j\theta} \cdot \frac{e^{\frac{j2\pi}{N}(n-m+\Delta fT)N} - 1}{e^{\frac{j2\pi}{N}(n-m+\Delta fT)} - 1} \\
 &= \frac{1}{N} \sum_{n=0}^{N-1} d_n e^{j\theta} \cdot \frac{e^{\frac{j2\pi}{N}(n-m+\Delta fT)\frac{N}{2}} \cdot e^{\frac{j2\pi}{N}(n-m+\Delta fT)\frac{N}{2}} - e^{-\frac{j2\pi}{N}(n-m+\Delta fT)\frac{N}{2}}}{e^{\frac{j2\pi}{N}(n-m+\Delta fT)\frac{1}{2}} \cdot e^{\frac{j2\pi}{N}(n-m+\Delta fT)\frac{1}{2}} - e^{-\frac{j2\pi}{N}(n-m+\Delta fT)\frac{1}{2}}} \quad (2.6)
 \end{aligned}$$

Therefore, we find the recovered data symbols are in the following form

$$y_m = \sum_{n=0}^{N-1} d_n e^{j\theta} e^{j\pi \frac{N-1}{N}(n-m+\Delta fT)} \cdot \frac{1}{N} \cdot \frac{\sin[\pi(n-m+\Delta fT)]}{\sin[(\pi/N) \cdot (n-m+\Delta fT)]} \quad (2.7)$$

From Eq.(2.7), we can see that recovered data symbols y_m will be equal to the actual data symbol, that is, $y_m = d_n$ for $m = n = 0, 1, 2, \dots, N-1$ if and only if the carrier phase θ , and the CFO Δf are zero; otherwise, the recovered data symbols will have distorted phases because of the exponential factor, $e^{j\theta} e^{j\pi \frac{N-1}{N}(n-m+\Delta fT)}$, and they will have lower magnitudes due to the

sinc function, $\frac{1}{N} \cdot \frac{\sin[\pi(n-m+\Delta fT)]}{\sin[(\pi/N) \cdot (n-m+\Delta fT)]}$. These distortions cause significant inter-carrier interference.

A very small frequency offset can lead to significant degradation in bit error rate (BER) performance. To maintain signal to interference ratios of 20dB or greater for the OFDM carriers, offset must be limited to 4% or less of the inter-carrier spacing [17]. This degradation is proportional to the number of subcarrier and signal to noise ratio (SNR). Therefore, CFO has to be corrected in the receiver in order to restore subcarrier orthogonality.

We can also derive a lower bound for the SNR at the output of the DFT (at the receiver part) for the OFDM carriers in a channel with AWGN and carrier frequency offset as follows;

If you consider the Eq.(2.7) without neglecting the w_k the received symbol

$$y_m = \sum_{n=0}^{N-1} d_n e^{j\theta} e^{j\pi \frac{N-1}{N}(n-m+\Delta fT)} \cdot \frac{1}{N} \cdot \frac{\sin[\pi(n-m+\Delta fT)]}{\sin[(\pi/N) \cdot (n-m+\Delta fT)]} + \sum_{k=0}^{N-1} w_k e^{-j \frac{2\pi mk}{N}} \quad (2.8)$$

Let, carrier phase offset $\theta = 0$ for convenience and if you look at the n^{th} element (i.e. $m = n$) of the received symbol consists of three different components;

$$y_{m=n} = (d_n h_n) \cdot \left(\frac{1}{N} \cdot \frac{\sin[\pi(\Delta fT)]}{\sin((\pi/N) \cdot (\Delta fT))} \right) \cdot e^{j\pi(\Delta fT) \left(\frac{N-1}{N} \right)} + I_n + W_n \quad (2.9)$$

The first component is the modulation value d_n modified by the channel transfer function. This component experiences an amplitude reduction and phase shift due to the frequency offset.

Let $\varepsilon = \Delta fT$ where, ε is the relative frequency offset of the channel (the ratio of the actual frequency offset to the inter-carrier spacing). Since N is always much greater than $\pi\varepsilon$, $N \cdot \sin(\pi\varepsilon/N)$ may be replaced by $\pi\varepsilon$.

The second term I_n is the ICI caused by the frequency offset and is given by

$$I_n = \sum_{\substack{l=0 \\ l \neq n}}^{N-1} (d_l h_l) \left\{ \frac{1}{N} \cdot \frac{\sin(\pi \varepsilon)}{\sin((\pi/N)(l-n+\varepsilon))} \right\} e^{j\pi \varepsilon \left(\frac{N-1}{N}\right)} e^{-j\pi \left(\frac{l-n}{N}\right)} \quad (2.10)$$

The third term W_n is due to the AWGN and is given by $W_n = \sum_{k=0}^{N-1} w_k e^{-j\frac{2\pi mk}{N}}$.

In order to evaluate the statistical properties of the ICI, some further assumptions are necessary. It is assumed that the modulation values have zero mean and are uncorrelated (i.e. $E[d_n] = 0$ and $E[d_n d_l^*] = |d|^2 \delta_{l,n}$), with this provision $E[I_n] = 0$, and

$$E[|I_n|^2] = |d|^2 \sum_{\substack{l=0 \\ l \neq n}}^{N-1} E(|h_l|^2) \cdot \left\{ \frac{(\sin(\pi \varepsilon))^2}{(N \cdot \sin((\pi/N) \cdot (l-n+\varepsilon)))^2} \right\} \quad (2.11)$$

The average channel gain, $E(|h_l|^2) = |h|^2$, is constant so above Eq.(2.11) can be written as Eq.(2.12)

$$E[|I_n|^2] = |d|^2 \cdot |h|^2 \cdot (\sin(\pi \varepsilon))^2 \cdot \sum_{\substack{p=-n \\ p \neq 0}}^{N-n-1} \left\{ \frac{1}{(N \cdot \sin((\pi/N) \cdot (p+\varepsilon)))^2} \right\} \quad (2.12)$$

The sum in Eq.(2.12) can be bounded for $\varepsilon = 0$. It consists of $N-1$ positive terms. The interval of the sum is contained within the longer interval $-(N-1) \leq p \leq (N-1)$, its location dependent on n . Also note the following; the argument of the sum is periodic with period N , it is an even function of p , and it is even about $p = N/2$. Thus the $N-1$ terms of the sum are a subset of the N terms in the intervals $-N/2 \leq p \leq 1$ and $1 \leq p \leq N/2$ for every n . Consequently,

$$\sum_{\substack{p=-n \\ p \neq 0}}^{N-n-1} \left\{ \frac{1}{(N \cdot \sin(\pi p/N))^2} \right\} < 2 \sum_{p=1}^{N/2} \left\{ \frac{1}{(N \cdot \sin(\pi p/N))^2} \right\} \quad (2.13)$$

Observe that $(\sin(\pi p/N))^2 \geq (2p/N)^2$ for $|p| \leq N/2$. Therefore,

$$2 \sum_{p=1}^{N/2} \frac{1}{(N \sin(\pi p/N))^2} < 2 \sum_{p=1}^{N/2} \frac{1}{(2p)^2} < \frac{1}{2} \sum_{p=1}^{\infty} \frac{1}{p^2} = \pi^2/12$$

upper bounds the sum for small ε . Numerically, we have determined that the sum in Eq.(2.12) is bounded by 0.5947 for $\varepsilon < 0.5$ so that

$$E[|I_n|^2] \leq 0.5947 |d|^2 |h|^2 (\sin \pi \varepsilon)^2; \quad |\varepsilon| \leq 0.5 \quad (2.14)$$

upper bounds the variance of the inter-carrier interference for values of carrier frequency offset up to plus or minus one half the carrier spacing.

Eq.(2.14) may be used to give a lower bound for the SNR at the output of the DFT for the OFDM carriers in a channel with AWGN and frequency offset. Thus,

$$SNR \geq \frac{|d|^2 |h|^2 \left\{ \frac{\sin(\pi \varepsilon)}{\pi \varepsilon} \right\}^2}{\left\{ 0.5947 |d|^2 |h|^2 (\sin \pi \varepsilon)^2 + E[|W_n|^2] \right\}} \quad (2.15)$$

It is easily established that $|d|^2 |h|^2 / E[|W_n|^2] = E_c / N_0$ where, E_c is the average received energy of the individual carriers and $N_0/2$ is the power spectral density of AWGN in the band pass transmission channel. Therefore, Eq.(2.15) may be more conveniently expressed as

$$SNR \geq \{E_c / N_0\} \cdot \left\{ \frac{\sin(\pi \varepsilon)}{\pi \varepsilon} \right\}^2 / \left\{ 1 + 0.5947 (E_c / N_0) (\sin \pi \varepsilon)^2 \right\} \quad (2.16)$$

with equality at $\varepsilon = 0$.

The simulation of the basic OFDM system performance with different values of CFO's at different values of SNR in AWGN channel is performed. SNR value of the subcarrier at the output of the DFT is calculated and its degradation effect due to increase in frequency offset value has been observed. Eq.(2.16) which will give the lower bound for the SNR at the output of the DFT for the OFDM subcarrier in a channel with AWGN and CFO is plotted

and compared with the practical OFDM system simulated. The simulated results are shown in section 2.4.

2.3 Moose Method

In [17], Moose proposed one of the earliest schemes to estimate the CFO. The method used by him is training sequence based. The training sequence is a known data sequence embedded in the preamble before transmitting data. After CFO is estimated at the receiver, the receiver removes the CFO in the received signal. This method applies two identical successive symbol sequences in the preamble. By using the property that CFO causes linear phase with respect to time, it estimates the CFO by comparing the phase offset between 2 identical successive sequences in the frequency domain at the receiver.

Here, the first OFDM symbol, or training symbol, is produced by doing FFT on a data sequence, d_n with $n = 0, 1, \dots, N-1$, and the second one by d_n with $n = N, N+1, \dots, 2N-1$. Both sequences are identical, that is $d_n = d_{n+N}$ for $n = 0, 1, \dots, N-1$. This method does not have any specific requirement for the content of these training sequences, as long as it avoids extreme average-to-peak power ratio. Therefore, we may select any pseudo noise code to be the training sequence.

Deriving from Eq.(2.1), we have the first and second OFDM symbols defined as

$$\begin{aligned} x_k &= \frac{1}{N} \sum_{n=0}^{N-1} d_n e^{j\frac{2\pi}{N}nk} & k = 0, 1, 2, \dots, N-1 \\ x_k &= \frac{1}{N} \sum_{n=N}^{2N-1} d_n e^{j\frac{2\pi}{N}nk} & k = N, N+1, N+2, \dots, 2N-1 \end{aligned} \quad (2.17)$$

We rearrange the index in Eq.(2.17). Let $n = n' + N$. It becomes

$$\begin{aligned} x_k &= \frac{1}{N} \sum_{n'=0}^{N-1} d_{n'+N} e^{j\frac{2\pi}{N}(n'+N)k} \\ &= \frac{1}{N} \sum_{n'=0}^{N-1} d_{n'+N} e^{j\frac{2\pi}{N}n'k} e^{j2\pi k} \end{aligned}$$

$$x_k = \frac{1}{N} \sum_{n'=0}^{N-1} d_{n'+N} e^{j\frac{2\pi}{N}n'k} \quad k = N, N+1, \dots, 2N-1 \quad (2.18)$$

Applying the channel model described previously, we find the received OFDM symbols are

$$r_k = \frac{1}{N} \sum_{n=0}^{N-1} h_n d_n e^{j\frac{2\pi}{N}nk} e^{j\theta} e^{j\frac{2\pi}{N}k\Delta T} + w_k \quad k = 0, 1, 2, \dots, N-1 \quad (2.19)$$

$$r_k = \frac{1}{N} \sum_{n=N}^{2N-1} h_n d_n e^{j\frac{2\pi}{N}nk} e^{j\theta} e^{j\frac{2\pi}{N}k\Delta T} + w_k \quad k = N, N+1, \dots, 2N-1 \quad (2.20)$$

Suppose $h_n = \delta_n$ for AWGN channel and neglect noise w_k for simplicity. Then, Eq.(2.20) becomes

$$r_k = x_k e^{j\theta} e^{j\frac{2\pi}{N}k\Delta T} \quad k = 0, 1, 2, \dots, 2N-1 \quad (2.21)$$

At the receiver, after FFT, the first and second recovered sequences become

$$y_{1,m} = \sum_{k=0}^{N-1} r_k e^{-j2\pi\frac{mk}{N}} \quad m = 0, 1, 2, \dots, N-1 \quad (2.22)$$

$$y_{2,m} = \sum_{k=N}^{2N-1} r_k e^{-j2\pi\frac{mk}{N}} \quad m = 0, 1, 2, \dots, N-1 \quad (2.23)$$

When we substitute Eq.(2.21) and Eq.(2.8) into Eq.(2.22), we have

$$\begin{aligned} y_{1,m} &= \sum_{k=0}^{N-1} r_k e^{-j2\pi\frac{mk}{N}} \quad m = 0, 1, 2, \dots, N-1 \\ &= \sum_{k=0}^{N-1} \left[\left(x_k e^{j\theta} e^{j2\pi\frac{\Delta T}{N}k} \right) e^{-j2\pi\frac{m}{N}k} \right] \\ &= \sum_{k=0}^{N-1} \left[\left(\frac{1}{N} \sum_{n=0}^{N-1} d_n e^{j2\pi\frac{n}{N}k} \right) e^{j\theta} e^{j2\pi\frac{\Delta T}{N}k} e^{-j2\pi\frac{m}{N}k} \right] \\ &= \frac{1}{N} \sum_{k=0}^{N-1} \sum_{n=0}^{N-1} d_n e^{j\theta} e^{j2\pi\frac{(n-m+\Delta T)}{N}k} \\ &= \frac{1}{N} \sum_{n=0}^{N-1} d_n e^{j\theta} \sum_{k=0}^{N-1} e^{j2\pi\frac{(n-m+\Delta T)}{N}k} \end{aligned}$$

Then it becomes

$$y_{1,m} = \sum_{n=0}^{N-1} d_n e^{j\theta} e^{j\pi \frac{N-1}{N} (n-m+\Delta fT)} \cdot \frac{1}{N} \cdot \frac{\sin \left[\pi (n-m+\Delta fT) \right]}{\sin \left[\frac{\pi}{N} (n-m+\Delta fT) \right]} \quad (2.24)$$

Also, substituting Eq.(2.21) and Eq.(2.19) into Eq.(2.22), we have

$$\begin{aligned} y_{2,m} &= \sum_{k=N}^{2N-1} r_k e^{-j2\pi \frac{mk}{N}} \quad m = 0, 1, 2, \dots, N-1 \\ &= \sum_{k=N}^{2N-1} \left[\left(x_k e^{j\theta} e^{j2\pi \frac{\Delta fT}{N} k} \right) e^{-j2\pi \frac{mk}{N}} \right] \\ &= \sum_{k=N}^{2N-1} \left[\left(\frac{1}{N} \sum_{n=0}^{N-1} d_{n+N} e^{j2\pi \frac{n}{N} k} \right) e^{j\theta} e^{j2\pi \frac{\Delta fT}{N} k} e^{-j2\pi \frac{mk}{N}} \right] \end{aligned}$$



Since the first and second training sequences are identical, that is, $d_n = d_{n+N}$ for $n = 0, 1, \dots, N-1$, so the final form is

$$\begin{aligned} y_{2,m} &= \frac{1}{N} \sum_{k=N}^{2N-1} \sum_{n=0}^{N-1} d_n e^{j\theta} e^{j2\pi \frac{(n-m+\Delta fT)}{N} k} \quad (2.25) \\ &= \frac{1}{N} \sum_{n=0}^{N-1} d_n e^{j\theta} \sum_{k'=0}^{N-1} e^{j2\pi \frac{(n-m+\Delta fT)}{N} (k'+N)} \quad \text{where, } k' = k - N \\ &= \frac{1}{N} \sum_{n=0}^{N-1} d_n e^{j\theta} \sum_{k'=0}^{N-1} e^{j2\pi \frac{(n-m+\Delta fT)}{N} k'} e^{j2\pi (n-m+\Delta fT)} \\ &= \frac{1}{N} \sum_{n=0}^{N-1} d_n e^{j\theta} e^{j2\pi (n-m+\Delta fT)} \sum_{k'=0}^{N-1} e^{j2\pi \frac{(n-m+\Delta fT)}{N} k'} \\ &= \frac{1}{N} \sum_{n=0}^{N-1} d_n e^{j\theta} e^{j2\pi (n-m+\Delta fT)} e^{j\pi \frac{N-1}{N} (n-m+\Delta fT)} \cdot \frac{\sin \left[\pi (n-m+\Delta fT) \right]}{\sin \left[(\pi/N) \cdot (n-m+\Delta fT) \right]} \\ &= \sum_{n=0}^{N-1} d_n e^{j\theta} e^{j2\pi (n-m)} e^{j2\pi \Delta fT} e^{j\pi \frac{N-1}{N} (n-m+\Delta fT)} \cdot \frac{1}{N} \cdot \frac{\sin \left[\pi (n-m+\Delta fT) \right]}{\sin \left[(\pi/N) \cdot (n-m+\Delta fT) \right]} \quad (2.26) \end{aligned}$$

Since $e^{j2\pi (n-m)} = 1$ for $n - m$ is a integer, Eq.(2.26) becomes

$$y_{2,m} = e^{j2\pi\Delta f T} \sum_{n=0}^{N-1} d_n e^{j\theta} e^{j\pi \frac{N-1}{N}(n-m+\Delta f T)} \cdot \frac{1}{N} \cdot \frac{\sin[\pi(n-m+\Delta f T)]}{\sin[(\pi/N)(n-m+\Delta f T)]} \quad (2.27)$$

Comparing Eq.(2.27) with Eq.(2.24), we see that the relationship between the first and second recovered training sequences is

$$y_{2,m} = e^{j2\pi\Delta f T} \cdot y_{1,m} \quad (2.28)$$

We rearrange the term in Eq.(2.28),

$$e^{j2\pi\Delta f T} = \frac{y_{2,m}}{y_{1,m}} = \frac{y_{2,m} \cdot y_{1,m}^*}{|y_{1,m}|^2} \quad (2.29)$$

where $(\cdot)^*$ denotes complex conjugate.

By using maximum likelihood estimation technique [17], the estimation of the CFO is defined as

$$\Delta \tilde{f} = \frac{1}{2\pi T} \tan^{-1} \left[\frac{\sum_{m=0}^{N-1} \text{Im}(y_{2,m} \cdot y_{1,m}^*)}{\sum_{m=0}^{N-1} \text{Re}(y_{2,m} \cdot y_{1,m}^*)} \right] \quad (2.30)$$

$$\hat{\varepsilon} = \frac{1}{2\pi} \tan^{-1} \left[\frac{\sum_{m=0}^{N-1} \text{Im}(y_{2,m} \cdot y_{1,m}^*)}{\sum_{m=0}^{N-1} \text{Re}(y_{2,m} \cdot y_{1,m}^*)} \right] \quad (2.31)$$

The performance of such estimators is usually measured by their closeness toward their Cramer-Rao lower bound (CRLB) (which will be discussed in section 3.5). For an unbiased estimator, the estimator's CRLB is bounded by its error variance. The CRLB for Moose's estimator [17] is defined by

$$\text{var}(\zeta) \geq \left(\frac{1}{2\pi} \right)^2 \cdot \frac{1}{N \cdot \text{SNR}} \quad (2.32)$$

where ζ is the error, N is the length of training sequence, and SNR is subcarrier energy to noise energy ratio. Moose's estimator is simple to use and efficient to implement. The estimated CFO is the angle of the correlation sum of the first and the second training sequences recovered at the receiver.

2.4 Simulation Results

2.4.1 Results for Performance of OFDM System with and without CFO

To simulate the OFDM system to obtain the performance of it in AWGN channel with and without CFO in MATLAB environment, we use the following simulation parameters;

- FFT size : $N = 256$
- Modulation scheme used: 8-PSK
- Channel used: Flat Channel
- Guard interval: $N_g = 64$
- Noise: AWGN
- No: of Monte Carlo simulations: 1000

Fig.2.3 shows the plot of SNR values at the output of the DFT for the OFDM subcarriers in a channel with AWGN and relative frequency offset varying from 0 to 0.5. Figure also contains the theoretical lower bound values of SNR at the output of the DFT for the OFDM subcarriers in a channel with AWGN and relative frequency offsets, which is given by Eq.(2.16). The graph is plotted for different SNR values of 11, 17, 23 and 29 dB varying the relative frequency offset value from 0 to 0.5. It can be observed from the plot that the practically obtained SNR values are above the theoretical lower bound SNR values.

2.4.2 Simulation Results of Moose Method

Fig.2.4 shows the simulation results for the estimate of relative frequency offset (i.e. $\hat{\epsilon}$) obtained using Moose method i.e. Eq.(2.31) verses actual value of frequency offset ϵ for E_c/N_0 values of 5 and 17 dB. The simulation parameters that are considered while performing simulations in MATLAB environment are as follows;

- FFT size : $N = 256$
- Modulation scheme used: 8-PSK
- Channel: Flat Channel
- Guard interval: $N_g = 64$
- Noise: AWGN

We observe from the plot that curve plotted using $E_c/N_0 = 5$ dB is varying more than the one plotted using $E_c/N_0 = 17$ dB. This tells us that as the E_c/N_0 value increases the variations in the curve decreases and it much more straight line.

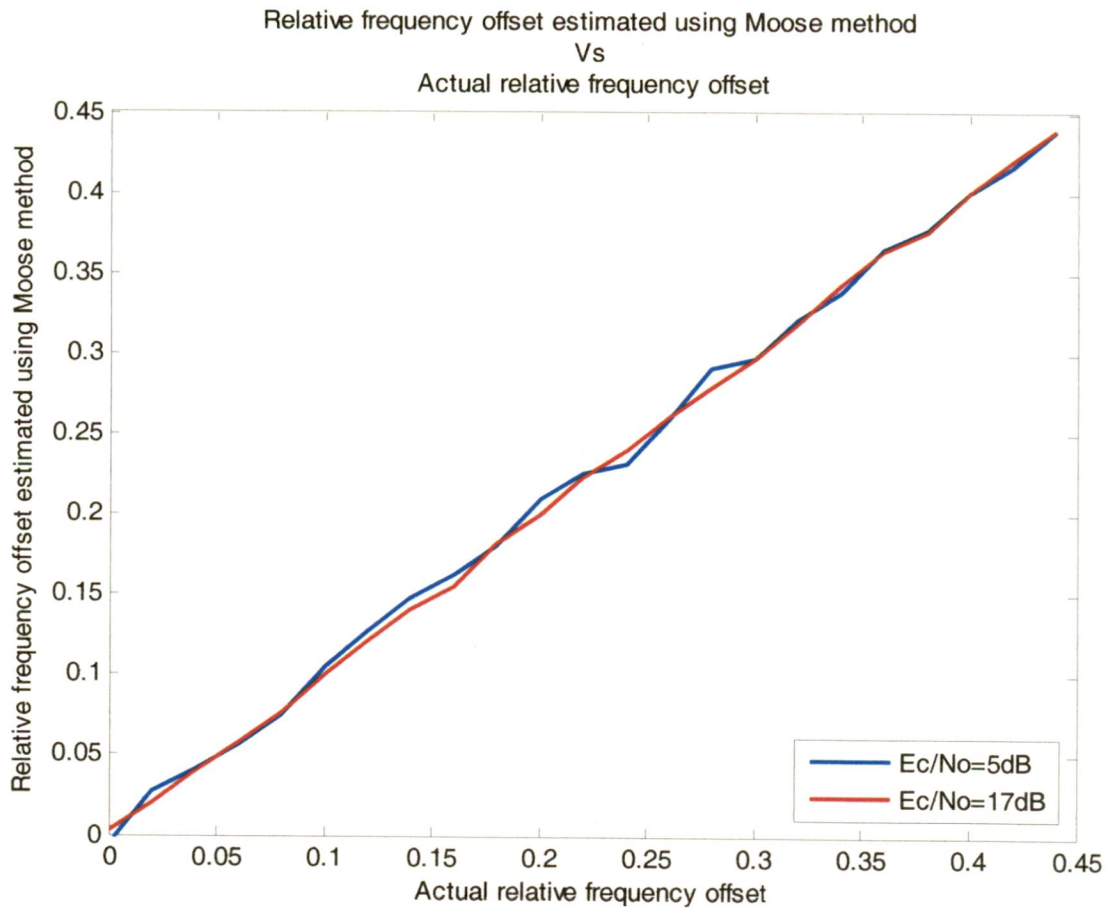


Fig.2.4 Relative frequency offset estimated using Moose method Vs Actual relative frequency offset for $E_c/N_0 = 5$ and 17 dB.

Chapter-3

Carrier frequency Offset Estimation in MIMO Systems

3.1 Introduction

Using multiple transmit and receive antennas in wireless fading channels has been advocated as a means to increase capacity and create diversity [18]. To exploit this possible increase of capacity and diversity, several coding and multiplexing schemes have been presented in literature. However, the performance of these schemes critically depends on the availability of accurate estimates of the synchronization parameters. In particular, carrier frequency offsets can substantially affect data detection. Moreover, the presence of a frequency offset is often detrimental in the estimation process of other parameters, such as the channel gains. Hence accurate frequency offset compensation in MIMO configuration is important to achieve a satisfactory performance.

Similar to SISO systems, ML frequency offset estimation using known training symbols in a MIMO context requires a numerical calculation, which is a time consuming task [19]. To overcome this inconvenience, some computationally efficient estimation techniques have been developed for SISO systems, which result in near optimum performance [20], [21]. They are even extended to MIMO systems. In the present chapter, we deal with some of the computationally efficient estimation techniques that are extended to a flat-fading MIMO configuration.

In this section, we deal with carrier frequency offset estimation for flat-fading Multiple-Input Multiple-Output channels using training symbols. Firstly we look at the traditional maximum likelihood (ML) frequency offset estimation method, which involves solving a maximization problem with no closed form solution. We consider both known and unknown channel cases. After that we will discuss one of the computationally efficient sub-optimal techniques of [22] along with its training sequence design. Finally we discuss about Cramer-Rao bound (CRB) and compare the simulated results.

3.2 System Model

Let us consider a flat fading MIMO channel with N_T transmit antennas and N_R receive antennas. We further assume that all transmit/receive antenna pairs are affected by the same frequency offset. This assumption is definitely valid for a frequency offset caused by an oscillator mismatch, since the different antennas can use a common oscillator or at least different collocated oscillators with a known and compensable difference. While considering the frequency offsets induced by Doppler shifts, they will be identical if the angles of arrival of different signals on the different antennas are identical [23].

Further, estimation and compensation of the mean Doppler shift, allows us to assume the channel to be quasi static as long as the block duration is smaller than the inverse of the remaining Doppler spread. We can model the MIMO system sampled at symbol rate as

$$\bar{y}_k = \mathbf{H}\bar{a}_k e^{j2\pi\Delta f T} + \bar{w}_k \quad k = 0, 1, \dots, L-1 \quad (3.1)$$

where

$\bar{y}_k = [y_k^n]_{n=1, \dots, N_R}^T$ is a $N_R \times 1$ vector of received signal samples

$\mathbf{H} = [h_{nm}]_{n=1, \dots, N_R, m=1, \dots, N_T}$ denotes the $N_R \times N_T$ channel matrix

h_{nm} are statistically independent and complex valued, with independent Gaussian zero mean real and imaginary parts, each having a variance of $1/2$; this yields $E[|h_{nm}|^2] = 1$.

$\bar{a}_k = [a_k^m]_{m=1, \dots, N_T}^T$ is a $N_T \times 1$ vector of known symbols with $E[|a_k^m|^2] = E_s$

Δf is the carrier frequency offset

$1/T$ is the symbol rate per transmit antenna

\bar{w}_k is a $N_R \times 1$ noise vector. The components of the noise vector are statistically independent and complex valued. All the real and imaginary parts are independent Gaussian variables with zero mean and variance $\sigma^2 = N_0/2$. The noise vectors at different instants of time are also statistically independent.

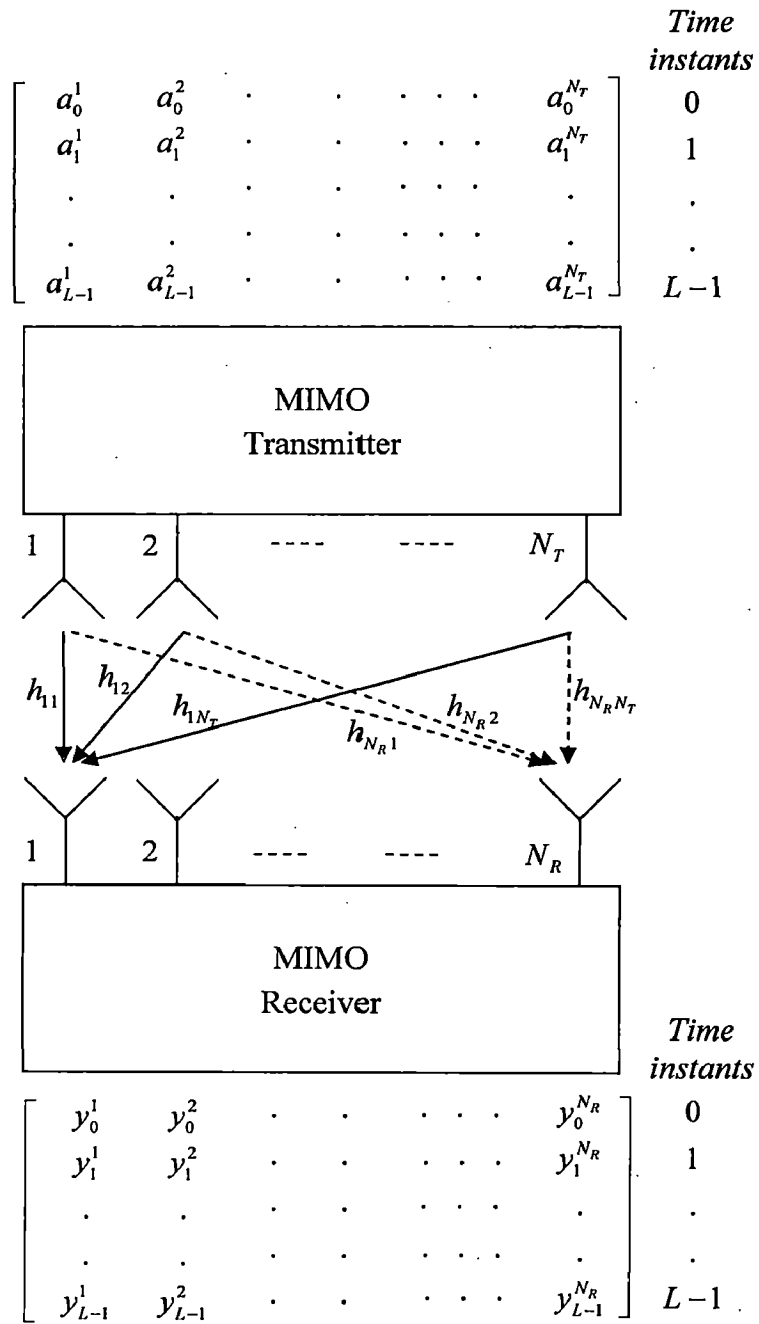


Fig. 3.1 $N_T \times N_R$ MIMO system model

In the following sections, we will consider the two cases;

1. CFO estimation methods using known training sequences when the *channel is known*.
2. CFO estimation methods using known training sequences when the *channel is unknown*.

CFO estimation when the channel is known is of no direct practical interest. This is not a realistic scenario, but it will turn out that the resulting algorithm is useful in the context of code-aided iterative joint estimation [23] of the frequency offset and the channel matrix, in which we assume no knowledge of the transmitted symbols at receiver side, yet information about the code structure is available.

3.3 CFO estimation with Known Channel

In this section, we will consider training sequence based CFO estimation methods assuming that the channel matrix \mathbf{H} to be known.

3.3.1 ML Estimation

The CFO estimation technique using ML method for AWGN SISO channels using a training sequence is well documented in literature [19]–[21]. When the MIMO channel matrix \mathbf{H} is considered to be known, a similar derivation as for SISO yields the following ML estimate [23]

$$\Delta\tilde{f}_{ML} = \arg \max_{\Delta\tilde{f}} \left| \sum_{k=0}^{L-1} y(k) e^{-j2\pi\Delta\tilde{f}kT} \right| \quad (3.2)$$

where $y(k) = \bar{\mathbf{a}}_k^H \mathbf{H}^H \bar{\mathbf{y}}_k$

Hence, the ML estimate maximizes the magnitude of the Fourier transform of $\{y(k)\}$. Unfortunately, a simple closed-form solution to the problem of maximizing Eq.(3.2) does not exist. The exact determination of the ML estimate from Eq.(3.2) would require a time consuming search over a large set of frequency values, making ML estimation computationally hard. It will be shown in simulation results (section 3.6), that for high signal to noise ratio, the Mean Square Error (MSE) of this estimate closely approaches the Cramer-Rao Lower Bound (CRLB), which is a theoretical lower bound on the MSE.

3.3.2 Computationally Efficient Estimation Method

To overcome the problem mentioned above (i.e. time consuming search over a larger set of frequency values), a number of sub-optimal closed-form frequency estimators have been discussed in the literature. One such a method [22] is discussed here. In Eq.(3.2) replacing the magnitude of the Fourier transform by its squared magnitude does not affect the value of the ML estimate. Rearranging the squared magnitude yields the following maximum likelihood expression:

$$\Delta\tilde{f}_{ML;S} = \arg \max_{\Delta\tilde{f}} \operatorname{Re} \left[\sum_{m=1}^{L-1} R(m) e^{-j2\pi\Delta\tilde{f}mT} \right] \quad (3.3)$$

where $R(m) = \sum_{k=m}^{L-1} y^*(k-m)y(m)$ is the time correlation

For convenience, decomposing $R(m)$ as the sum of a useful terms that is independent of the AWGN noise \bar{w}_k , and a noise term caused by \bar{w}_k . We get

$$R(m) = A(m) \exp(j2\pi\Delta f m T) + \text{noise} \quad (3.4)$$

where $A(m)$ is a positive real quantity, given by

$$A(m) = \sum_{k=m}^{L-1} |\mathbf{H}\bar{a}_k|^2 |\mathbf{H}\bar{a}_{k-m}|^2 \quad (3.5)$$

Setting the derivative (with respect to $\Delta\tilde{f}$) of the function to be maximized in Eq.(3.3) equal to zero, the ML estimate satisfies the following equation:

$$\operatorname{Im} \left[\sum_{m=1}^{L-1} m R(m) e^{-j2\pi m \Delta\tilde{f} T} \right] = 0 \quad (3.6)$$

Above Eq.(3.6) can be equivalently written as

$$\sum_{m=1}^{L-1} \left[m |R(m) \sin(\arg(R(m)) - 2\pi m \Delta\tilde{f} T) \right] = 0 \quad (3.7)$$

Assuming that the training sequence is sufficiently long, the first term in Eq.(3.4) is strongly dominating, in which case $\arg(R(m)) \cong 2\pi m \Delta f T$. Hence it follows from Eq.(3.7) that $\Delta\tilde{f} = \Delta f$, so that the argument of the sinc function in Eq.(3.7) is small.

Using in Eq.(3.7) the approximation $\sin(x) \cong x$ for $|x| \ll 1$ yields the following Eq.(3.8) with respect to $\Delta\tilde{f}$.

$$\sum_{m=1}^{L-1} \left[m |R(m)| (\arg(R(m)) - 2\pi m \Delta\tilde{f} T) \right] = 0 \quad (3.8)$$

Grouping terms appropriately and limiting the summation interval to $[1, M]$ with $M \leq L-1$, to reduce complexity furthermore, the new closed form frequency estimator is obtained:

$$\Delta\tilde{f}_{ML,S} = \frac{1}{2\pi T} \frac{\sum_{m=1}^M m |R(m)| \arg(R(m))}{\sum_{m=1}^M m^2 |R(m)|} \quad (3.9)$$

We should indicate that because of the presence of $\arg(\cdot)$ function in Eq.(3.9), $\Delta\tilde{f}_{ML,S}$ is ambiguous when $|\arg(R(m))|$ exceeds π . This limits the operating range of the proposed frequency offset estimation technique to the interval $|\Delta f| < [2MT]^{-1}$. Simulation results of this method simulated for 4 x 1 and 4 x 2 MIMO system are shown in section 3.6.

3.4 CFO Estimation with Unknown Channel

In this section, we will consider training sequence based joint maximum likelihood estimation of channel and carrier frequency offset assuming that the channel matrix \mathbf{H} to be unknown

3.4.1 Joint ML estimation of the Channel and CFO

Let us consider the Log Likelihood Function (LLF) of \mathbf{H} and Δf from the observations of Eq.(3.1), we get

$$\ln p(\mathbf{Y}/\mathbf{H}, \Delta f) = -\frac{1}{N_0} \sum_{k=0}^{L-1} \left| \bar{y}_k - \mathbf{H} \bar{\mathbf{a}}_k e^{j2\pi \Delta f k T} \right|^2 \quad (3.10)$$

The joint ML estimate corresponds to the values of \mathbf{H} and Δf that maximize $\ln p(\mathbf{Y}/\mathbf{H}, \Delta f)$. For a given trial value $\Delta\tilde{f}$, the channel matrix $\tilde{\mathbf{H}}$ that maximizes Eq.(3.10)

is readily found to be Eq.(3.12). Inserting Eq.(3.12) in Eq.(3.10) and rearranging yields the $\Delta\tilde{f}$ estimate Eq.(3.11).

$$\Delta\tilde{f}_{ML;H} = \arg \max_{\Delta\tilde{f}} \operatorname{Re} \left[\sum_{m=1}^{L-1} R_H(m) e^{-j2\pi m \Delta\tilde{f} T} \right] \quad (3.11)$$

$$\tilde{\mathbf{H}}_{ML;H} = \left(\sum_{k=0}^{L-1} \bar{y}_k \bar{a}_k^H e^{-j2\pi \Delta\tilde{f}_{ML;H} k T} \right) \left(\sum_{n=0}^{L-1} \bar{a}_n \bar{a}_n^H \right)^{-1} \quad (3.12)$$

where $R_H(m) = \sum_{k=m}^{L-1} \bar{y}_{k-m}^H \bar{y}_k \mathbf{A}(k, k-m)$ and (3.13)

$$\mathbf{A}(k, l) = \bar{a}_k^H \left(\sum_{n=0}^{L-1} \bar{a}_n \bar{a}_n^H \right) \bar{a}_l \quad (3.14)$$

The closed form solution to the maximization problem of Eq.(3.11) does not exist. Exact determination of $\Delta\tilde{f}_{ML;H}$ requires a time consuming numerical search which makes frequency offset estimation a computationally hard problem. On the other hand, the channel estimation algorithm Eq.(3.12) requires only a small computational effort once the CFO estimate has been found. Hence it is of practical interest to search for a CFO estimation algorithm with reduced complexity, avoiding the exhaustive search implied in Eq.(3.11).

3.4.2 Computationally Efficient Estimation Method

To overcome the problem mentioned above, a number of sub-optimal closed-form joint CFO and channel matrix estimators have been discussed in the literature. One such a method [22] is discussed here.

Considering the similarity between Eq.(3.3) and Eq.(3.11), closed form approximation to Eq.(3.11) and Eq.(3.12) can be given by Eq.(3.15) and Eq.(3.16) respectively

$$\Delta\tilde{f}_{ML;H;S} = \frac{1}{2\pi T} \frac{\sum_{m=1}^{L-1} m |R_H(m)| \arg [R_H(m)]}{\sum_{m=1}^{L-1} m^2 |R_H(m)|} \quad (3.15)$$

$$\tilde{\mathbf{H}}_{ML;H;S} = \left(\sum_{k=0}^{L-1} \bar{y}_k \bar{a}_k^H e^{-j2\pi \Delta\tilde{f}_{ML;H;S} k T} \right) \left(\sum_{n=0}^{L-1} \bar{a}_n \bar{a}_n^H \right)^{-1} \quad (3.16)$$

As it will be shown in simulation results, in contrast with the algorithm Eq.(3.9) for the known channel case, the performance of the approximated closed form solution Eq.(3.15) does not approach the CRB at high SNR for an arbitrary training sequence. We observe an error floor in the MSE performance of the closed form estimator Eq.(3.15), where as the ML estimator Eq.(3.11) does not suffer from such floor.

If we examine Eq.(3.13), and separating signal from noise terms we can write Eq.(3.13) as

$$R_H(m) = C(m) \exp(j2\pi\Delta fmT) + noise \quad (3.17)$$

$$\text{where } C(m) = \sum_{k=m}^{L-1} \bar{a}_{k-m}^H \mathbf{H}^H \mathbf{H} \bar{a}_k \mathbf{A}(k, k-m) \quad (3.18)$$

It is important to note that $C(m)$ is generally complex valued. Considering the phase of the time correlation, we can distinguish three terms:

$$\arg(R_H(m)) = 2\pi\Delta fmT + \phi_d(m) + \phi_n(m) \quad (3.19)$$

First term in Eq.(3.19) corresponds to the phase rotation caused by the frequency offset; Second term $\phi_d(m) = \arg(C(m))$ is a self noise term, and the last term $\phi_n(m)$ is introduced by noise. It is apparent that the approximation

$$\arg(R_H(m)) \cong 2\pi\Delta fmT \quad (3.20)$$

that is crucial in obtaining Eq.(3.15) is less accurate when $\phi_d(m) + \phi_n(m)$ takes a larger values. This is the reason for the discrepancy between the performance of the sub-optimal solution Eq.(3.15) and the ML performance. Following remarks can be made observing the above discussion:

- For systems with a single transmit antenna ($N_T = 1$), it is readily seen from Eq.(3.18) that $C(m)$ is real valued, and no self noise term $\phi_d(m)$ appears. This illustrates that the self-noise is induced by the multiple transmit antenna set up.
- For systems with more than one transmit antenna, $C(m)$ is generally not real, resulting in a self noise term $\phi_d(m)$. Consequently, even in the absence of noise, the approximation Eq.(3.20) is not valid, and an error floor is observed.

- When the number L of randomly selected pilot symbols increases, the error floor reduces. This effect is readily understood since, for large L , $C(m)$ converges to its expectation $E_a[C(m)]$, which is real-valued.
- The ML estimation Eq.(3.11) does not suffer from an error floor, which might be unexpected since the time correlation in Eq.(3.11) contains the self noise term $\phi_d(m)$. However, $\Delta\tilde{f}_{ML;H} = \Delta f$ in the absence of noise. This is clearly not true for $\Delta\tilde{f}_{ML;H} = \Delta f$, indicating that the self noise term $\phi_d(m)$ is too large for the approximation Eq.(3.20) to be accurate.

3.4.3 Training Sequence Design

By proper design of the training sequence we can eliminate this self noise and the resulting MSE floor. The basic cause of this self noise is due to $C(m)$ being complex valued. So to make $C(m)$ real valued the following proposition is constituted.

Proposition 1: $C(m)$ is real valued $\forall m$ if every symbol vector \bar{a}_k is chosen from a complete orthogonal set, i.e. $\bar{a}_k \in \{\bar{a}_0, \bar{a}_1, \dots, \bar{a}_{N_T-1}\} \forall k$, with $\alpha_i^H \alpha_j = N_T E_s \delta_{i-j}$, and every vector α_j is chosen at least once.

Accordingly, the self noise term $\phi_d(m) = \arg(C(m))$ in Eq.(3.19) equals zero and the error floor disappears. We point out that the number of symbol vectors in the orthogonal set is equal to the number of transmit antennas N_T .

In order to optimize the training sequence furthermore, we take the training sequence constraint, which minimizes the MSE of the channel estimate, into account. In [25], the training sequence that minimizes the MSE related to the ML estimation of the channel matrix \mathbf{H} is orthogonal across all transmit antennas, i.e. the different rows of the matrix $[\bar{a}_0, \bar{a}_1, \dots, \bar{a}_{L-1}]$ should be orthogonal, which means that

$$\sum_k \bar{a}_0 \bar{a}_k^H = L E_s \mathbf{I} \quad (3.21)$$

where \mathbf{I} is the identity matrix.

Let us consider a periodic training sequence consisting of K systematic repetitions of the N_T orthogonal symbol vectors ($L = KN_T$).

$$\bar{a}_{iN_T+j} = \bar{a}_j, \quad i = 0, 1, \dots, K-1, \quad j = 0, 1, \dots, N_T-1 \quad (3.22)$$

With above training sequence, no error floor will occur and Eq.(3.21) is satisfied. Due to periodicity, $R_H(m)$ is zero except for indices $m = kN_T, k \in \mathbb{N}$ yielding a significant complexity reduction since only these non-zero terms have to be taken into account in the computation of Eq.(3.15). To reduce complexity furthermore, we can limit the summation interval in Eq.(3.15) to $[1, MN_T]$, with $M < K$. Using the above discussed training sequence in Eq.(3.15) and after some simplification we get

$$\Delta \tilde{f}_{ML;H} = \sum_{n=1}^M B_n \arg(r(n)) \quad (3.23)$$

$$\text{where } r(n) = \sum_{k=nN_T}^{L-1} \bar{y}_{k-nN_T}^H \bar{y}_k \quad (3.24)$$

$$B_n = \frac{1}{2\pi N_T T} \frac{n(K-n)}{\sum_{n=1}^M (K-n)n^2} \quad (3.25)$$

Because of the presence of the $\arg(\cdot)$ function in Eq.(3.23), its operating range is limited to $|\Delta f| < [2MN_T T]^{-1}$.

3.5 Cramer-Rao Lower Bound

In this section we will have discussion on Exact Cramer-Rao Bound and its importance. In estimation theory and statistics, the Cramer-Rao bound (CRB) or Cramer-Rao Lower Bound (CRLB), named in honor of Harald Cramer and Callyampudi Radhakrishna Rao who were among the first to derive it [26], will expresses a lower bound on the variance of estimators of a deterministic parameter.

In its simplest form, the bound states that the variance of any unbiased estimator is at least as high as the inverse of the Fisher Information Matrix (FIM). An unbiased estimator which achieves this lower bound is said to be efficient. Such a solution achieves the lowest possible mean squared error among all unbiased methods, and is therefore the Minimum

Variance Unbiased (MVU) estimator. However, in some cases, no unbiased technique exists which achieves the bound. This may occur even when an MVU estimator exists.

Suppose η is an unknown deterministic scalar parameter which is to be estimated from X measurements, distributed according to some probability density function $f(X;\eta)$. The variance of any unbiased estimator $\hat{\eta}$ of η is then bounded by the inverse of the Fisher Information $I(\eta)$. Where, the Fisher information $I(\eta)$ is defined by

$$I(\eta) = E \left[\left(\frac{\partial \log(f(X;\eta))}{\partial \eta} \right)^2 \right] = -E \left[\frac{\partial^2 \log(f(X;\eta))}{\partial \eta^2} \right] \quad (3.26)$$

The efficiency of an unbiased estimator $\hat{\eta}$, measures how close this estimator's variance comes to CRLB; estimator efficiency is defined as

$$\text{efficiency}(\hat{\eta}) = \frac{I(\eta)^{-1}}{\text{var}(\hat{\eta})} \leq 1 \quad (3.27)$$

Now if we consider multivariate case (i.e. when the parameter to be estimated is vector $\bar{\eta}$), which contains the channel gains and frequency offsets as the estimation parameters, then CRLB for estimation of channel gains and estimation of frequency offsets can be obtained as follows;

Let the vector to be estimated be denoted by $\bar{\eta}$ from ' N ' observation values. It contains N_R parameters to be estimated each belonging to one of the receive antenna. Each of this parameter again contains real and imaginary parts of channel gain and frequency offset

$$\bar{\eta} = [\bar{\eta}_1 \quad \dots \quad \bar{\eta}_{N_R}]^T \quad (3.28)$$

$$\text{with } \bar{\eta}_k = [\text{Re}(\bar{h}_k)^T \quad \text{Im}(\bar{h}_k)^T \quad \bar{\omega}_k^T]^T \quad (3.29)$$

$$\text{Channel gains } \bar{h}_k = [h_{k1} \quad \dots \quad h_{kN_T}]^T \quad (3.30)$$

$$\text{Frequency offsets } \bar{\omega}_k = [\omega_{k1} \quad \dots \quad \omega_{kN_T}]^T \quad (3.31)$$

Proposition: The Fisher Information Matrix (FIM) for the estimation of $\bar{\eta}$ is block-diagonal, i.e.

$$\mathbf{F} = \begin{bmatrix} \mathbf{F}_1 & & & & \\ & \mathbf{F}_2 & & & \\ & & \ddots & & \\ & & & \ddots & \\ & & & & \mathbf{F}_{N_R} \end{bmatrix} \quad (3.32)$$

where each \mathbf{F}_k is the FIM corresponding to the estimation of $\bar{\eta}_k$ and is given by

$$\mathbf{F}_k = \frac{2}{\sigma^2} \begin{bmatrix} \text{Re}(\mathbf{U}_k) & -\text{Im}(\mathbf{U}_k) & -\text{Im}(\mathbf{T}_k) \\ \text{Im}(\mathbf{U}_k) & \text{Re}(\mathbf{U}_k) & \text{Re}(\mathbf{T}_k) \\ -\text{Im}(\mathbf{T}_k)^T & \text{Re}(\mathbf{T}_k)^T & \text{Re}(\mathbf{V}_k) \end{bmatrix} \quad (3.33)$$

where $\mathbf{U}_k = \mathbf{A}_{\omega_k}^H \mathbf{A}_{\omega_k}$, $\mathbf{T}_k = \mathbf{A}_{\omega_k}^H \mathbf{D}_k \mathbf{A}_{\omega_k} \mathbf{D}(\bar{h}_k)$ and $\mathbf{V}_k = \mathbf{D}^H(\bar{h}_k) \mathbf{A}_{\omega_k}^H \mathbf{D}_k^2 \mathbf{A}_{\omega_k} \mathbf{D}(\bar{h}_k)$ with

$$\mathbf{A}_{\omega_k} = \begin{bmatrix} a_1^1 e^{j\omega_{k1}} & a_1^2 e^{j\omega_{k2}} & \dots & \dots & \dots & a_1^{N_T} e^{j\omega_{kN_T}} \\ a_2^1 e^{j2\omega_{k1}} & a_2^2 e^{j2\omega_{k2}} & \dots & \dots & \dots & a_2^{N_T} e^{j2\omega_{kN_T}} \\ \vdots & \vdots & \vdots & \vdots & \vdots & \vdots \\ a_N^1 e^{jN\omega_{k1}} & a_N^2 e^{jN\omega_{k2}} & \dots & \dots & \dots & a_N^{N_T} e^{jN\omega_{kN_T}} \end{bmatrix} \quad (3.34)$$

$$\mathbf{D}(\bar{h}_k) = \text{diag}(\bar{h}_k) \quad (3.35)$$

$$\mathbf{D}_k = \text{diag}(1, 2, \dots, N) \quad (3.36)$$

The CRB for the estimation of $\bar{\eta}_k$ is obtained as the inverse of \mathbf{F}_k and can be written as

$$\begin{aligned} \text{CRB}(\bar{\eta}_k) &= \frac{\sigma^2}{2} \begin{bmatrix} \text{Re}(\mathbf{U}_k^{-1}) & -\text{Im}(\mathbf{U}_k^{-1}) & \mathbf{0} \\ \text{Im}(\mathbf{U}_k^{-1}) & \text{Re}(\mathbf{U}_k^{-1}) & \mathbf{0} \\ \mathbf{0} & \mathbf{0} & \mathbf{0} \end{bmatrix} \\ &+ \frac{\sigma^2}{2} \begin{bmatrix} \text{Im}(\mathbf{U}_k^{-1} \mathbf{T}_k) \\ -\text{Re}(\mathbf{U}_k^{-1} \mathbf{T}_k) \\ \mathbf{I} \end{bmatrix} \text{Re}(\mathbf{W}_k)^{-1} \times \begin{bmatrix} \text{Im}(\mathbf{U}_k^{-1} \mathbf{T}_k)^T & -\text{Re}(\mathbf{U}_k^{-1} \mathbf{T}_k)^T & \mathbf{I} \end{bmatrix} \quad (3.37) \end{aligned}$$

with $\mathbf{W}_k = \mathbf{V}_k - \mathbf{T}_k^H \mathbf{U}_k^{-1} \mathbf{T}_k$.

Observations:

The following observations can be made from the above expression

- Since the FIM is block-diagonal, CRB is also block-diagonal and this decouples the estimation errors corresponding to the parameters of two different Rx antennas. This implies that the estimation of the parameters of interest can be carried out independently for each receive antenna.
- The CRB for the estimation of \bar{h}_k can be given as

$$CRB(\bar{h}_k) = \frac{\sigma^2}{2} \left\{ 2\mathbf{U}_k^{-1} - \mathbf{U}_k^{-1} \mathbf{T}_k [\text{Re}(\mathbf{W}_k)]^{-1} \mathbf{T}_k^H \mathbf{U}_k^{-1} \right\} \quad (3.38)$$

- The CRB for the estimation $\bar{\omega}_k$ can be given as

$$CRB(\bar{\omega}_k) = \frac{\sigma^2}{2} \left\{ \text{Re}(\mathbf{V}_k - \mathbf{T}_k^H \mathbf{U}_k^{-1} \mathbf{T}_k) \right\}^{-1} \quad (3.39)$$

- The CRB for the estimation of \bar{h}_k and $\bar{\omega}_k$ depends on all $\{h_{kl}\}_{l=1}^{N_r}$ through the matrices $\mathbf{D}(\bar{h}_k)$.
- The CRB for the estimation of \bar{h}_k and $\bar{\omega}_k$ also depends on all $\{\omega_{kl}\}_{l=1}^{N_r}$; more precisely, it depends on the differences $\omega_{kl} - \omega_{kq}$; when all the frequency offsets at the k^{th} receive antenna are equal i.e. $\omega_{kl} = \omega_{kq} = \omega_k$, the CRB for estimation of the k^{th} frequency offset no longer depends on ω_k . Indeed, \mathbf{A}_{ω_k} (Eq.(3.34)) becomes

$$\mathbf{A}_{\omega_k} = \text{diag}(e^{j\omega_k}, \dots, e^{jN\omega_k}) \mathbf{Z} \quad (3.40)$$

$$\text{where } \mathbf{Z} = [\bar{a}_0^T, \bar{a}_1^T, \dots, \bar{a}_N^T]^T \quad (3.41)$$

and the matrices $\mathbf{U}_k, \mathbf{T}_k$ and \mathbf{V}_k only depends on . Furthermore, Eq.(3.37) can be represented as

$$CRB \left(\begin{bmatrix} \bar{h}_k \\ \bar{\omega}_k \end{bmatrix} \right) = \frac{\sigma^2}{2} \begin{bmatrix} 2(\mathbf{Z}^H \mathbf{Z})^{-1} + \gamma_k^{-1} \bar{\beta}_k \bar{\beta}_k^H & -j\gamma_k^{-1} \bar{\beta}_k \\ j\gamma_k^{-1} \bar{\beta}_k^H & \gamma_k^{-1} \end{bmatrix} \quad (3.42)$$

$$\text{where } \bar{\beta}_k = (\mathbf{Z}^H \mathbf{Z})^{-1} \mathbf{Z}^H \mathbf{D}_k \mathbf{Z} \bar{h}_k \quad (3.43)$$

$$\text{and } \gamma_k = \bar{h}_k^H \mathbf{Z}^H \mathbf{D}_k \left(\mathbf{I} - \mathbf{Z} (\mathbf{Z}^H \mathbf{Z})^{-1} \mathbf{Z}^H \right) \mathbf{D}_k \mathbf{Z} \bar{h}_k \quad (3.44)$$

The exact CRB (i.e. finite sample), although obtained in Eq.(3.42) is in closed form, exhibits a rather complicated dependence with respect to the channel gains and frequency offsets. Thus it does not provide immediate insights into the influence of the channel on the estimation accuracy. So, we consider asymptotic CRB (i.e. large sample) which will be a much simpler function of \bar{h}_k and $\bar{\omega}_k$.

In order to obtain the asymptotic CRB, we assume that $\{a_i^\mu\}$ are realizations of zero-mean stationary random processes, and we examine the limiting behavior of the FIM. Under this mild condition on $\{a_i^\mu\}$, the asymptotic CRB for the estimation of $\bar{\eta}_k$ can be written as

$$\lim_{N \rightarrow \infty} \mathbf{J}_N \text{CRB}(\bar{\eta}) \mathbf{J}_N^T = \frac{\sigma^2}{2} \begin{bmatrix} 2\mathbf{R}_k^{-1} + 3\mathbf{D}(\bar{h}_k)\Gamma_k^{-1}\mathbf{D}^H(\bar{h}_k) & -6j\mathbf{D}(\bar{h}_k)\Gamma_k^{-1} \\ 6j\Gamma_k^{-1}\mathbf{D}^H(\bar{h}_k) & 12\Gamma_k^{-1} \end{bmatrix} \quad (3.45)$$

$$\text{where } \mathbf{J}_N = \begin{bmatrix} N^{1/2}\mathbf{I}_n & \mathbf{0} \\ \mathbf{0} & N^{3/2}\mathbf{I}_n \end{bmatrix}, [\mathbf{R}_k]_{pq} = E\left\{\left(a_p'\right)^* \left(a_q'\right)\right\} \delta(\omega_{kp}, \omega_{kq})$$

$$\Gamma_k = \text{Re}\left(\mathbf{D}^H(\bar{h}_k)\mathbf{R}_k\mathbf{D}(\bar{h}_k)\right)$$

Eq.(3.45) is a simple expression of the asymptotic CRB as a function of the channel gains and the correlation properties of the training sequence. It should be observed that the asymptotic CRB no longer depends on the values of ω_{kl} ; it only depends on whether they are equal or not. Furthermore, when the random processes a_p' and a_q' are uncorrelated more precisely, it suffices that $E\left(\left(a_p'\right)^* \left(a_q'\right)\right) = 0$ for $p \neq q$ or when, $\omega_{kp} \neq \omega_{kq}$ for all $p \neq q$, the matrix \mathbf{R}_k becomes real valued and diagonal, and the asymptotic CRB takes the very simple form

$$\lim_{N \rightarrow \infty} \mathbf{J}_N \text{CRB}(\bar{\eta}) \mathbf{J}_N^T = \frac{\sigma^2}{2} \begin{bmatrix} 5\mathbf{R}_k^{-1} & -6j\mathbf{R}_k^{-1}\mathbf{D}^H(\bar{h}_k) \\ 6j\mathbf{D}^{-1}(\bar{h}_k)\mathbf{R}_k^{-1} & 12\mathbf{D}^{-1}(\bar{h}_k)\mathbf{R}_k^{-1}\mathbf{D}^H(\bar{h}_k) \end{bmatrix} \quad (3.46)$$

$$\text{where } \mathbf{R}_k = \text{diag}(P_1, P_2, \dots, P_{N_r}) \text{ with } P_l = E\left\{|a_p'|^2\right\}$$

Eq.(3.46) implies that

$$\text{asCRB}(h_{kl}) = \frac{5\sigma^2}{2NP_l} \quad (3.47)$$

$$asCRB(\omega_{kl}) = \frac{6\sigma^2}{N^3 P_l |h_{kl}|^2} \quad (3.48)$$

We will also show that asymptotic CRB of Eq.(3.46) is close to the exact CRB of Eq.(3.42) even for small number of sample observations 'N' by simulations in Section 3.6.

3.6 Simulation Results

3.6.1 Simulation Results of Exact CRB and Asymptotic CRB

To illustrate the fact that the asymptotic CRB closely approximates the exact CRB, even when training sequence length N is small, we considered the SISO system as example for simulating in MATLAB environment as follows;

- Channel impulse response which consists of six paths as

$$h(k) = \sum_{n=0}^5 A_n g(kT_s - \tau_n - t_0)$$

Where A_n : are the attenuation of each path with variances $\{-3,0,-2,-6,-8,10\}$ dB,

τ_n/T_s : Normalized delays are selected as $\{0, 0.054, 0.135, 0.432, 0.621, 1.351\}$.

Furthermore $t_0 = 3T_s$ and $g(t)$ is a raised cosine with rolloff of 0.5.

- Frequency offset is set to $\Delta f = 0.08$ and noise power is selected as $10 \log_{10} 1/\sigma_w^2 = 10dB$.
- The exact CRB and asymptotic CRB are computed for 2000 Monte Carlo trials. In each trial, signal is generated with different random training sequence and different AWGN noise.

Fig.3.2 shows the asymptotic CRB values of frequency offset and mean, minimum and maximum of exact CRB values of frequency offset for different lengths of training sequences. From the plot we can notice that as the length of training sequence increases asymptotic CRB approaches the Exact CRB values. We can also observe that even for very small training sequence lengths (i.e. at $N=20$) we can claim that asymptotic CRB approximates exact CRB.

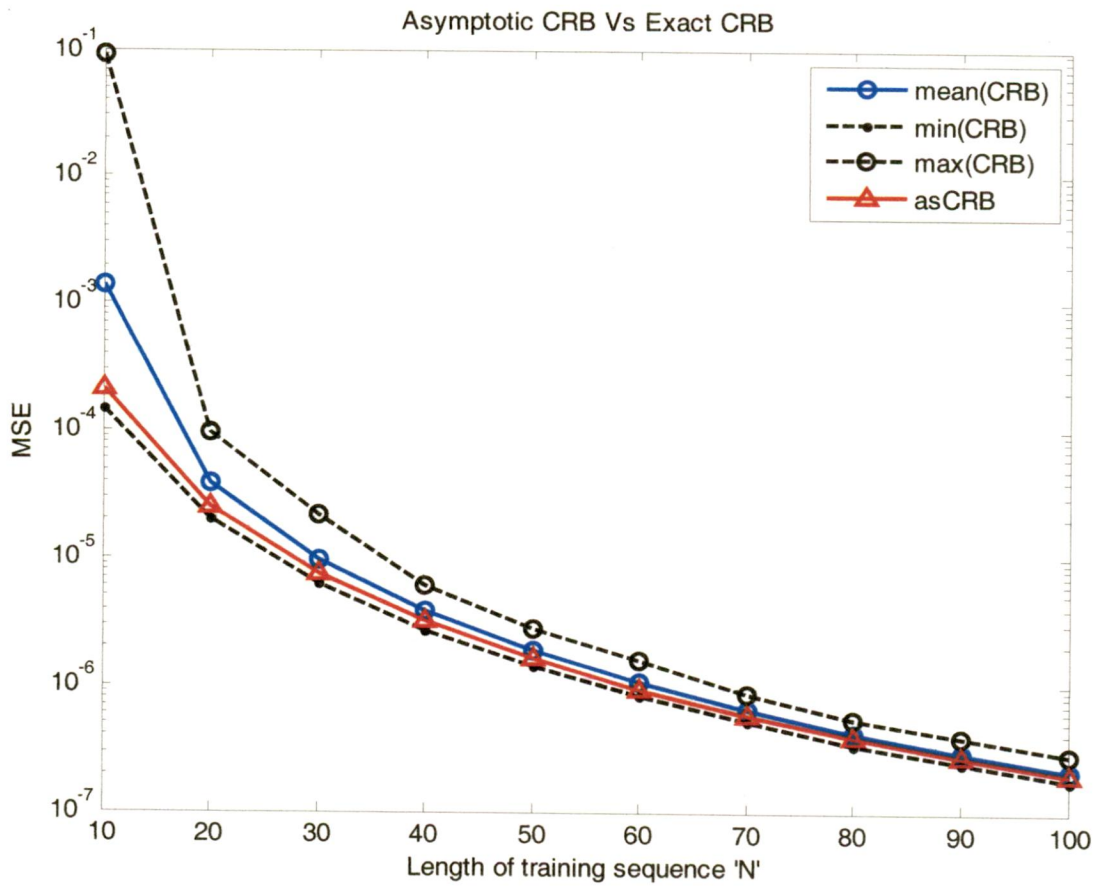


Fig.3.2 Comparison of Exact CRB and Asymptotic CRB for different training sequence lengths

3.6.2 Simulation Results of CFO Estimation with Known Channel (Using Pseudo Random Sequence as training sequence)

To simulate the ML estimation method and computationally efficient CFO estimation method with known channel for MIMO systems those are discussed in sections 3.3.1 and 3.3.2 respectively. The simulation parameters used are as follows;

- Assumption : *All transmit/receive antenna pairs are affected by same CFO*
- No. of Transmit antennas : $N_T = 4$
- No. of Receive antennas : $N_R = 1$ or 2
- Training sequence used : *Pseudo random sequence*
- Length of training sequence : $L = 20$
- Channel used : *Flat fading channel*
- Modulation scheme used : *QAM modulation*
- SNR values taken : $\{-10, -5, 0, 5, 10, 15, 20\}$ dB
- No. of Monte Carlo simulation trials : 10^6 trials (i.e. 10^6 OFDM symbols)

Fig.3.3 shows the Mean Square Error (MSE) results of the computationally intensive ML estimation method and computationally efficient estimation method for 4 x 1 MIMO system. It also contains the Cramer-Rao Lower Bound (CRLB) as the bench mark showing the lowest value that cannot be crossed by any unbiased estimator.

Fig.3.4 shows the MSE results of the computationally intensive ML estimation method and computationally efficient estimation method for 4 x 2 MIMO system. It also contains the Cramer-Rao Lower Bound (CRLB).

Fig.3.5 shows the MSE performance of both 4 x 1 and for 4 x 2 MIMO systems in one plot.

From Fig.3.3 and Fig.3.4 we can observe that computationally efficient estimation method approaches the ML estimation method or CRLB (which are almost close to each other) as the SNR value increases.

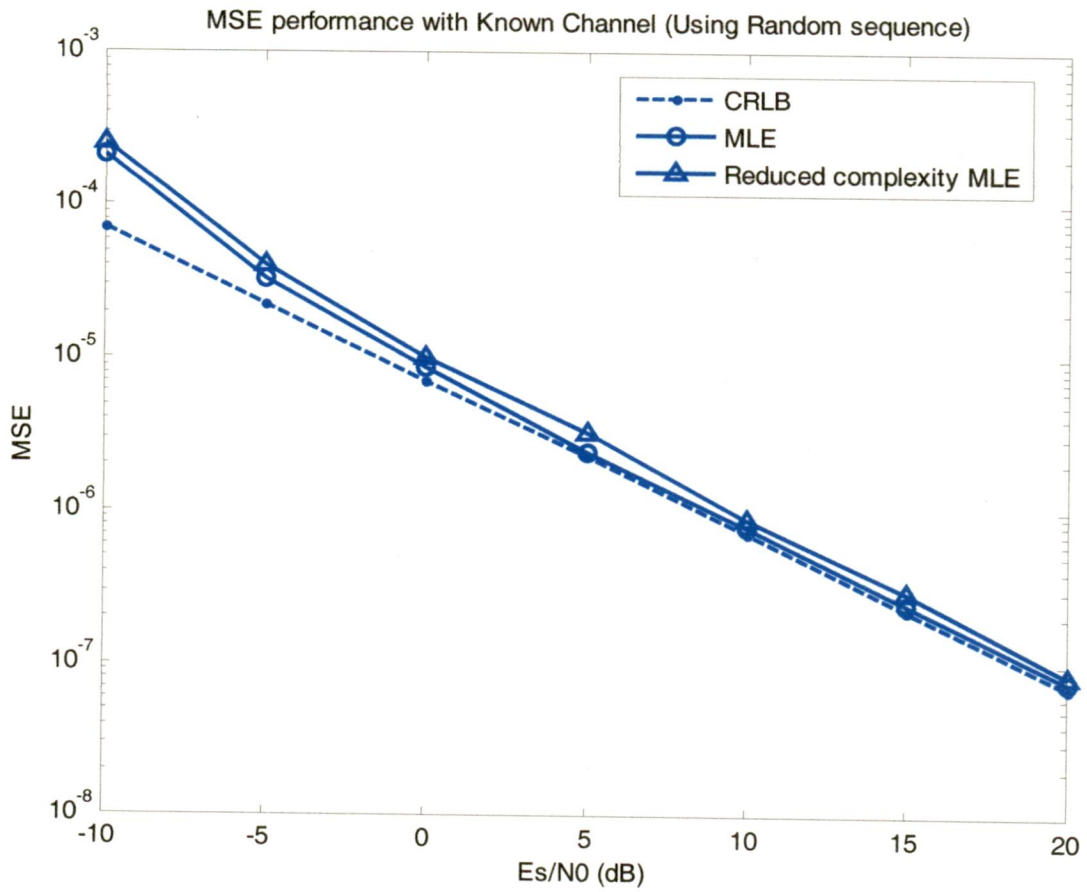
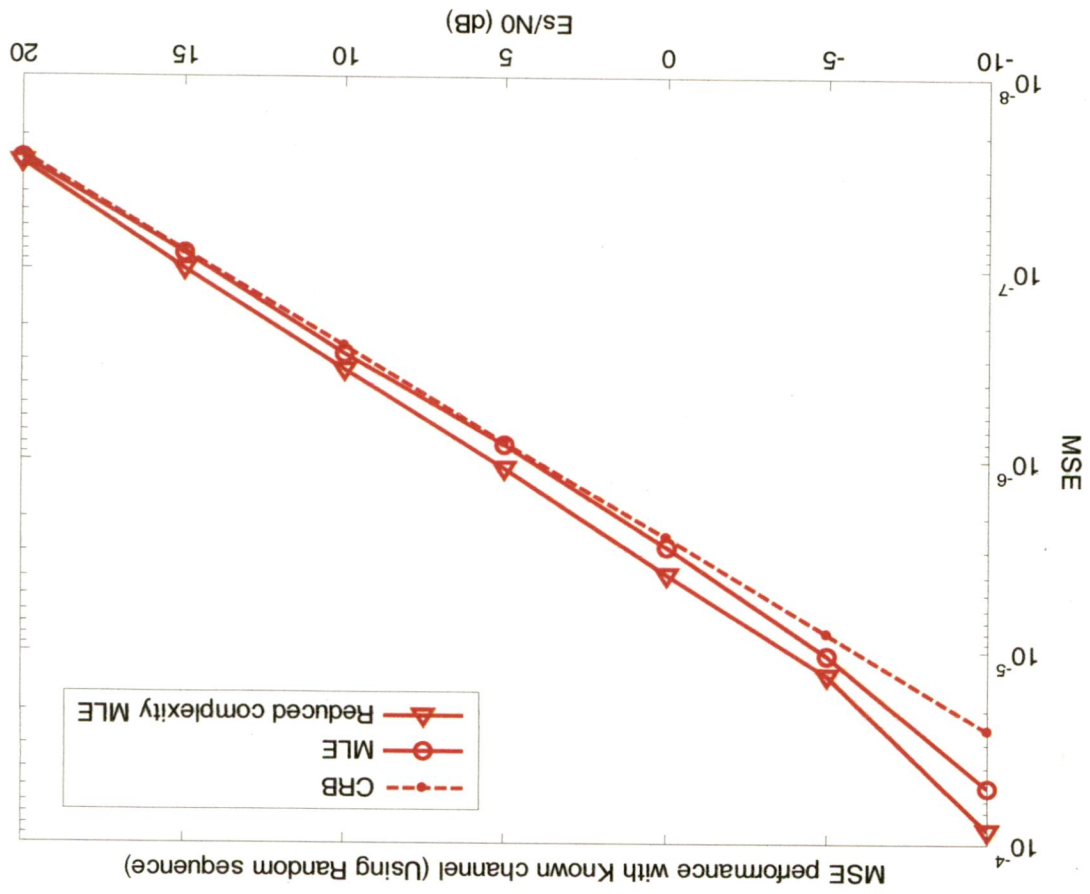


Fig.3.3 Comparison of MSE performance of MLE method and Reduced complexity MLE method simulated for 4 x 1 MIMO system (using pseudo random sequence as training sequence and when channel is known)

Fig.3.4 Comparison of MSE performance of MLE method and Reduced complexity MLE method simulated for 4 X 2 MIMO system (using pseudo random sequence as training sequence and when channel is known)



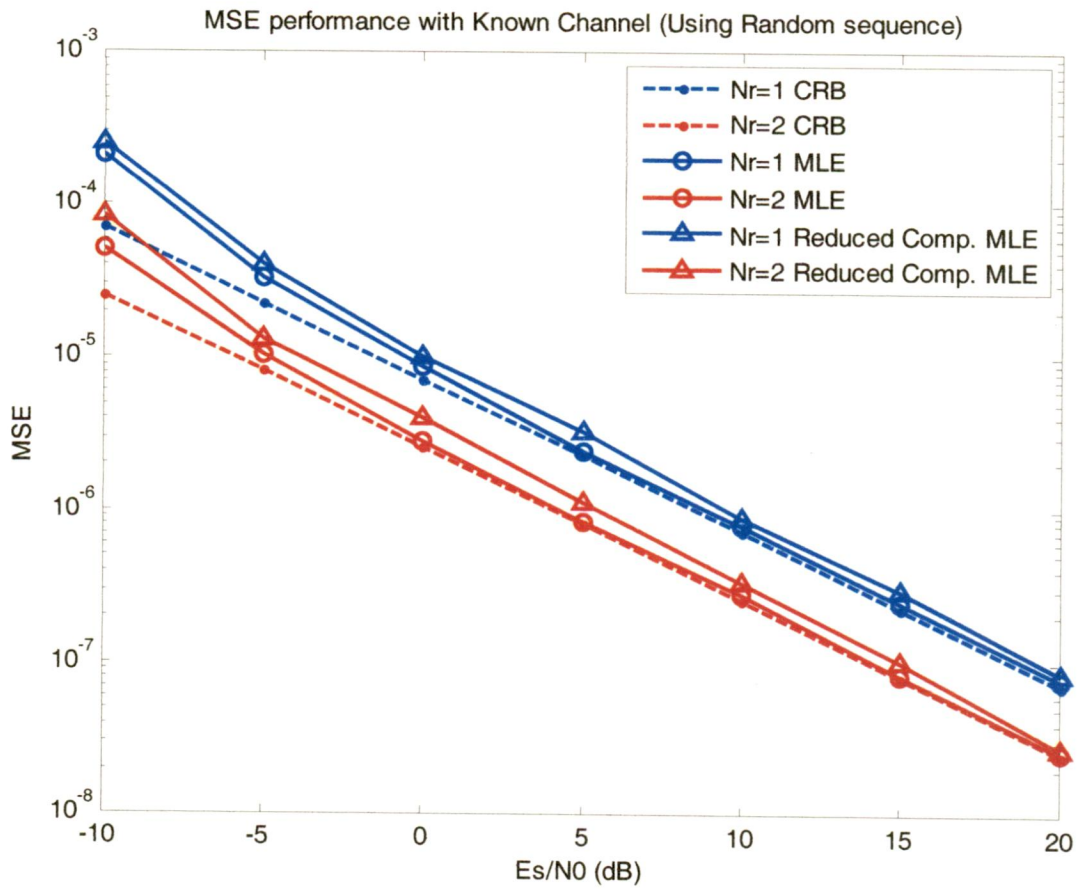


Fig.3.5 Comparison of MSE performance of MLE method and Reduced complexity MLE method simulated for 4 x 1 and 4 x 2 MIMO system (using pseudo random sequence as training sequence and when channel is known)

3.6.3 Simulation Results of CFO Estimation with Unknown Channel (Using Pseudo Random Sequence as training sequence)

To simulate the ML estimation method and computationally efficient CFO estimation method with unknown channel for MIMO systems those are discussed in sections 3.4.1 and 3.4.2 respectively. The simulation parameters used are as follows;

- Assumption : *All transmit/receive antenna pairs are affected by same CFO*
- No. of Transmit antennas : $N_T = 4$
- No. of Receive antennas : $N_R = 1$ or 2
- Training sequence used : *Pseudo random sequence*
- Length of training sequence : $L = 20$
- Channel used : *Flat fading channel*
- Modulation scheme used : *QAM modulation*
- SNR values taken : $\{-10, -5, 0, 5, 10, 15, 20\}$ dB
- No. of Monte Carlo simulation trials : 10^6 trials (i.e. 10^6 OFDM symbols)

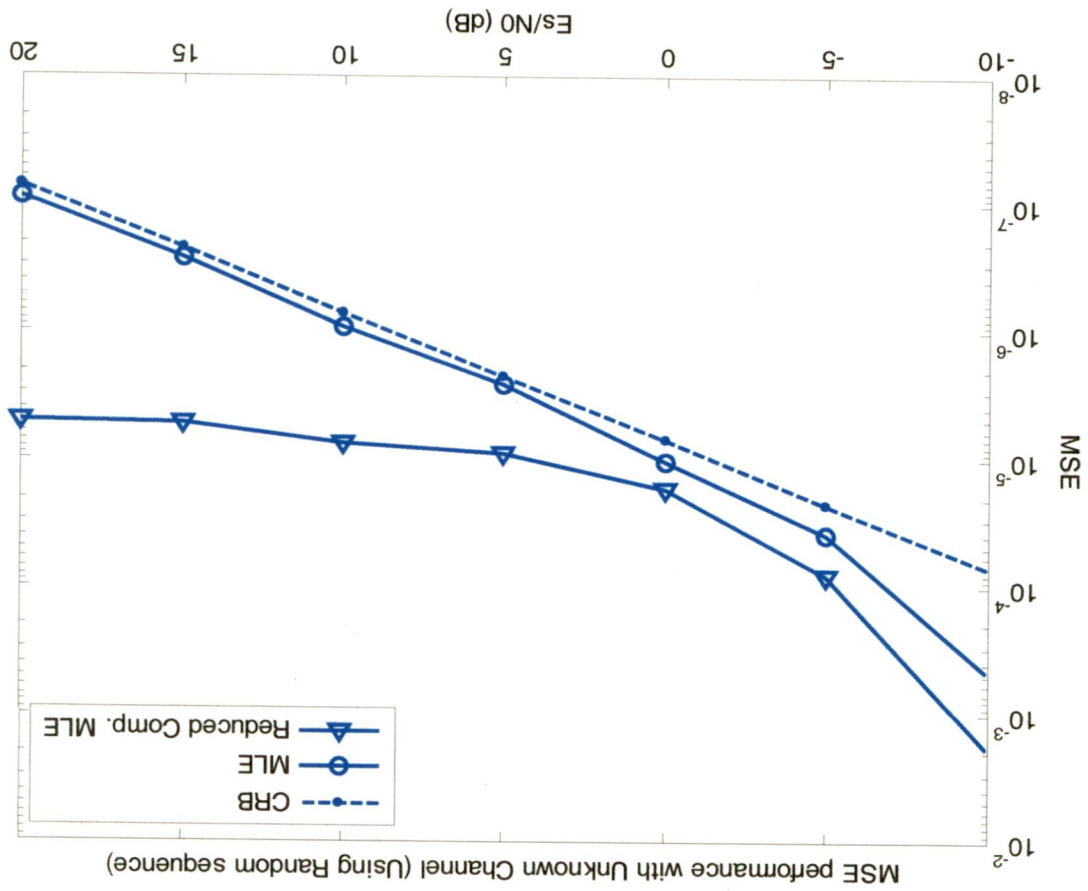
Fig.3.6 shows the MSE results of the computationally intensive ML estimation method and computationally efficient estimation method for 4 x 1 MIMO system when channel is unknown. CRLB is also plotted as bench mark for convenience.

Fig.3.7 shows the MSE results of the computationally intensive ML estimation method and computationally efficient estimation method for 4 x 2 MIMO system when the channel is unknown.

Fig.3.5 shows the MSE performance of both 4 x 1 and for 4 x 2 MIMO systems when channel is unknown in one plot.

From Fig.3.6 and Fig.3.7 we can observe that computationally efficient estimation method does not approach the ML estimation method or CRLB (which are almost close to each other) as the SNR value increases. At initial values of SNR it will try to approach the ML estimate but after reaching a particular minimum, it will not reduce further due to the noise floor created by the random training sequence transmitted by other transmit antennas.

Fig.3.6 Comparison of MSE performance of MLE method and Reduced complexity MLE method simulated for 4 X 1 MIMO system (using pseudo random sequence as training sequence and when channel is Unknown)



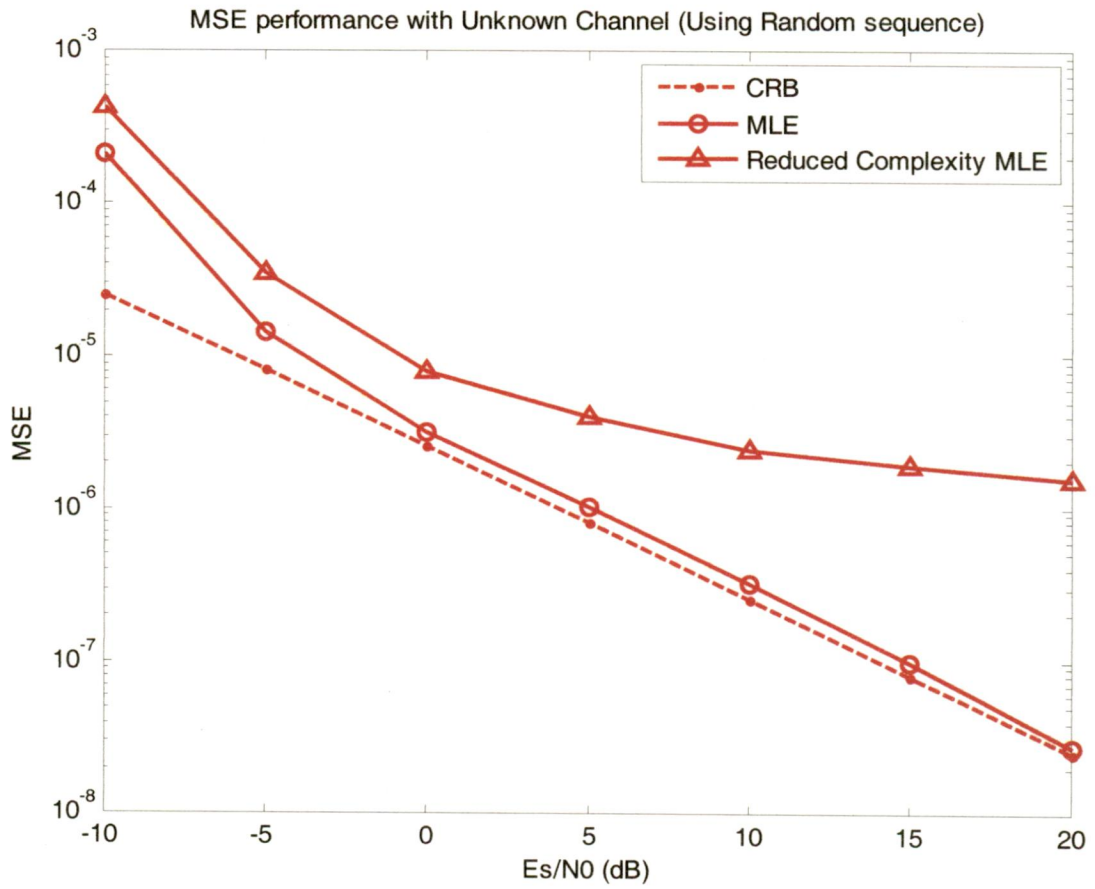


Fig.3.7 Comparison of MSE performance of MLE method and Reduced complexity MLE method simulated for 4 x 2 MIMO system (using pseudo random sequence as training sequence and when channel is Unknown)

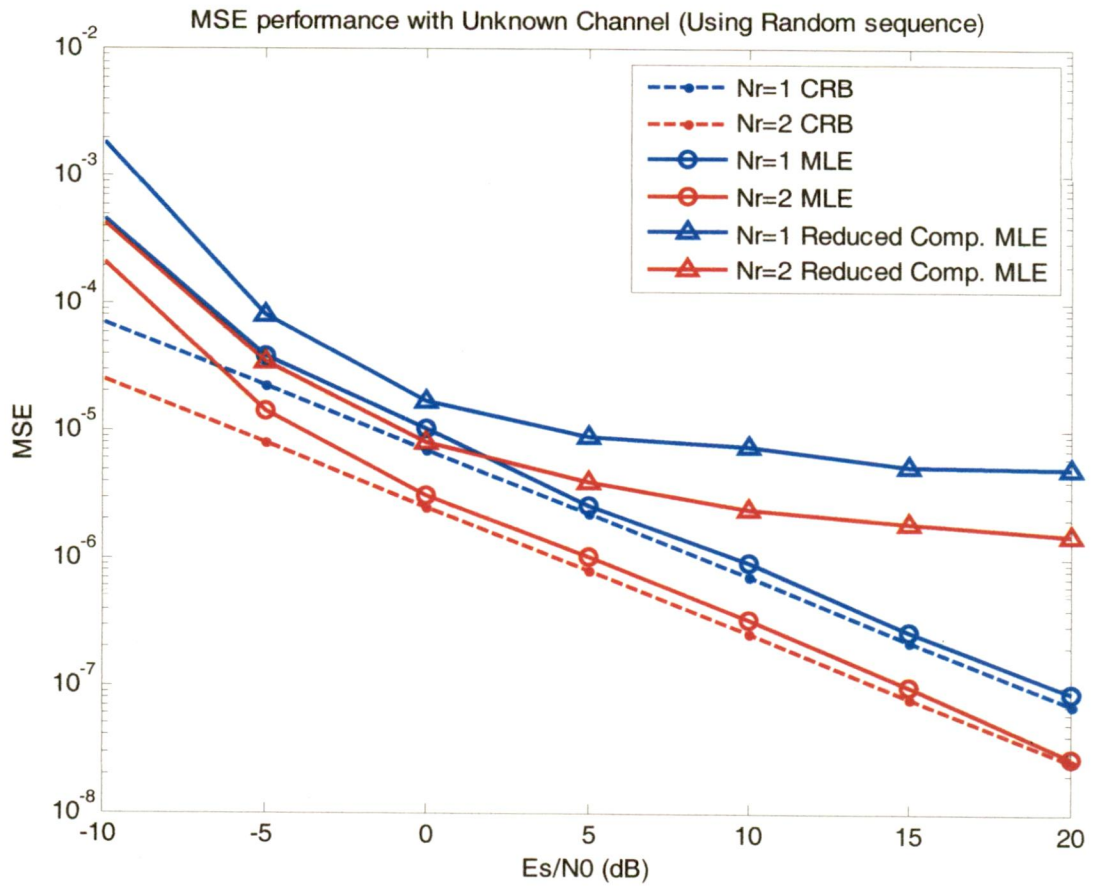


Fig.3.8 Comparison of MSE performance of MLE method and Reduced complexity MLE method simulated for 4 x 1 and 4 x 2 MIMO system (using pseudo random sequence as training sequence and when channel is Unknown)

3.6.4 Simulation Results of CFO Estimation with Unknown Channel (Using Orthogonal Sequence as training sequence)

Simulations performed in this section use the Orthogonal training sequences instead of pseudo random training sequences that are used in previous section. The simulation parameters used are as follows;

- Assumption : *All transmit/receive antenna pairs are affected by same CFO*
- No. of Transmit antennas : $N_T = 4$
- No. of Receive antennas : $N_R = 1$ or 2
- Training sequence used : *Pseudo random sequence*
- Length of training sequence : $L = 20$
- Channel used : *Flat fading channel*
- Modulation scheme used : *QAM modulation*
- SNR values taken : $\{-10, -5, 0, 5, 10, 15, 20\}$ dB
- No. of Monte Carlo simulation trials : 10^6 trials (i.e. 10^6 OFDM symbols)

Fig.3.9 shows the MSE results of the computationally intensive ML estimation method and computationally efficient estimation method for 4 x 1 MIMO system when channel is unknown (using Orthogonal training sequences).

Fig.3.10 shows the MSE results of the computationally intensive ML estimation method and computationally efficient estimation method for 4 x 2 MIMO system when the channel is unknown (using Orthogonal training sequences).

Fig.3.11 shows the MSE performance of both 4 x 1 and for 4 x 2 MIMO systems when channel is unknown (using Orthogonal training sequences) in one plot.

From Fig.3.9 and Fig.3.10 we can observe that computationally efficient estimation method approaches the ML estimation method or CRLB as the SNR value increases. This is due to the use of Orthogonal training sequences, which will not produce any noise floor as training sequences are Orthogonal to each other and not interfere to each other while estimation process.

Fig.3.12 shows the MSE performance of computationally efficient estimation method of both 4 x 1 and 4 x 2 MIMO systems using pseudo random sequence and orthogonal sequence

as training sequences. From the plot we can notice the performance improvement in using orthogonal training sequences.

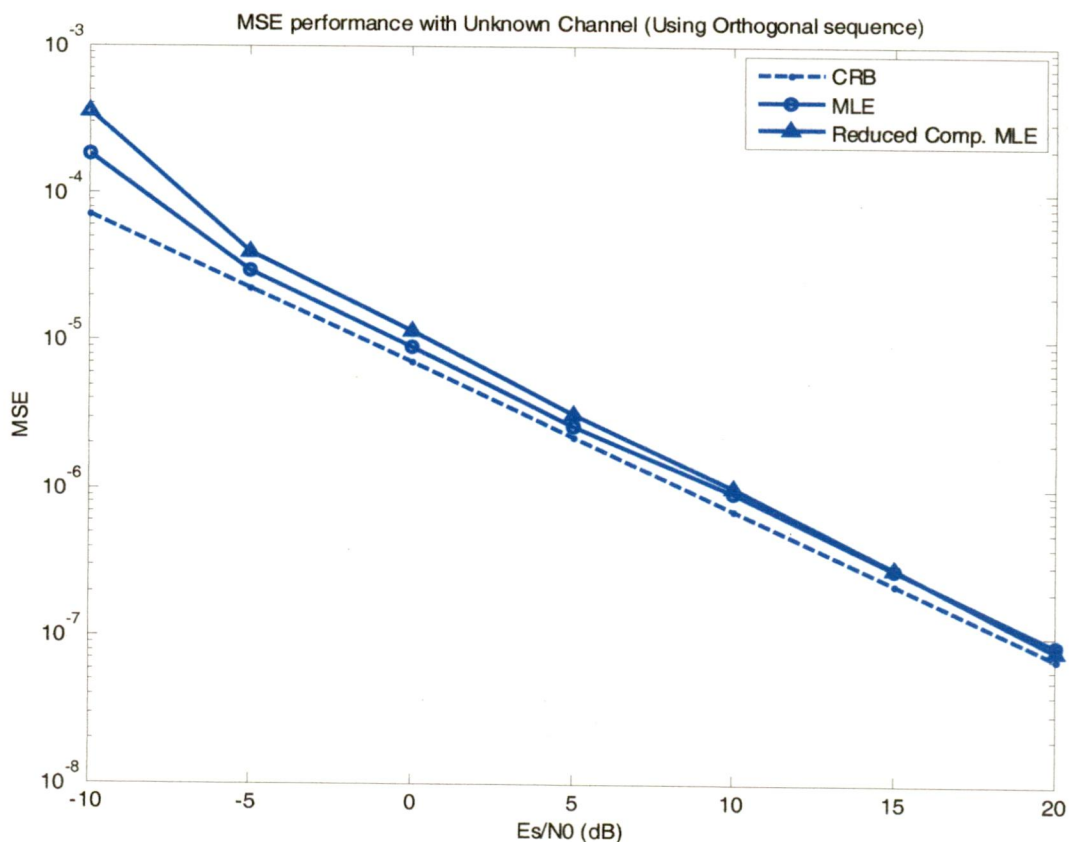


Fig.3.9 Comparison of MSE performance of MLE method and Reduced complexity MLE method simulated for 4 x 1 MIMO system (using Orthogonal sequence as training sequence and when channel is Unknown)

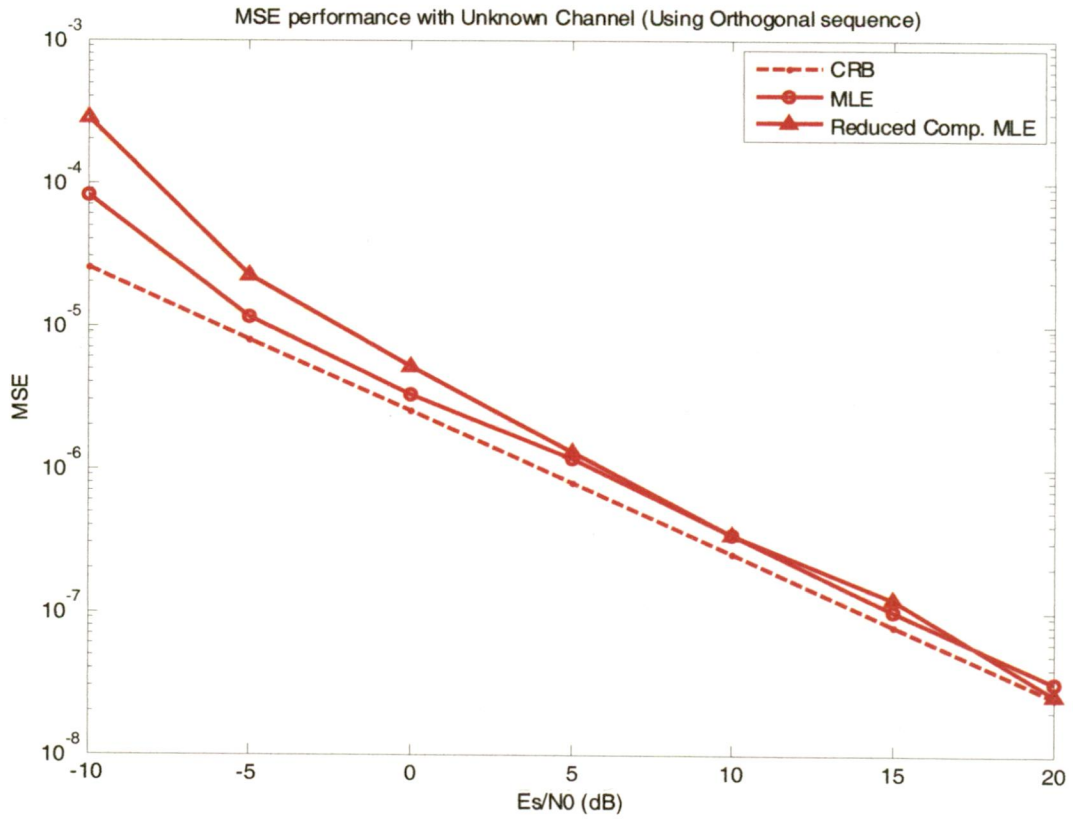


Fig.3.10 Comparison of MSE performance of MLE method and Reduced complexity MLE method simulated for 4 x 2 MIMO system (using Orthogonal sequence as training sequence and when channel is Unknown)

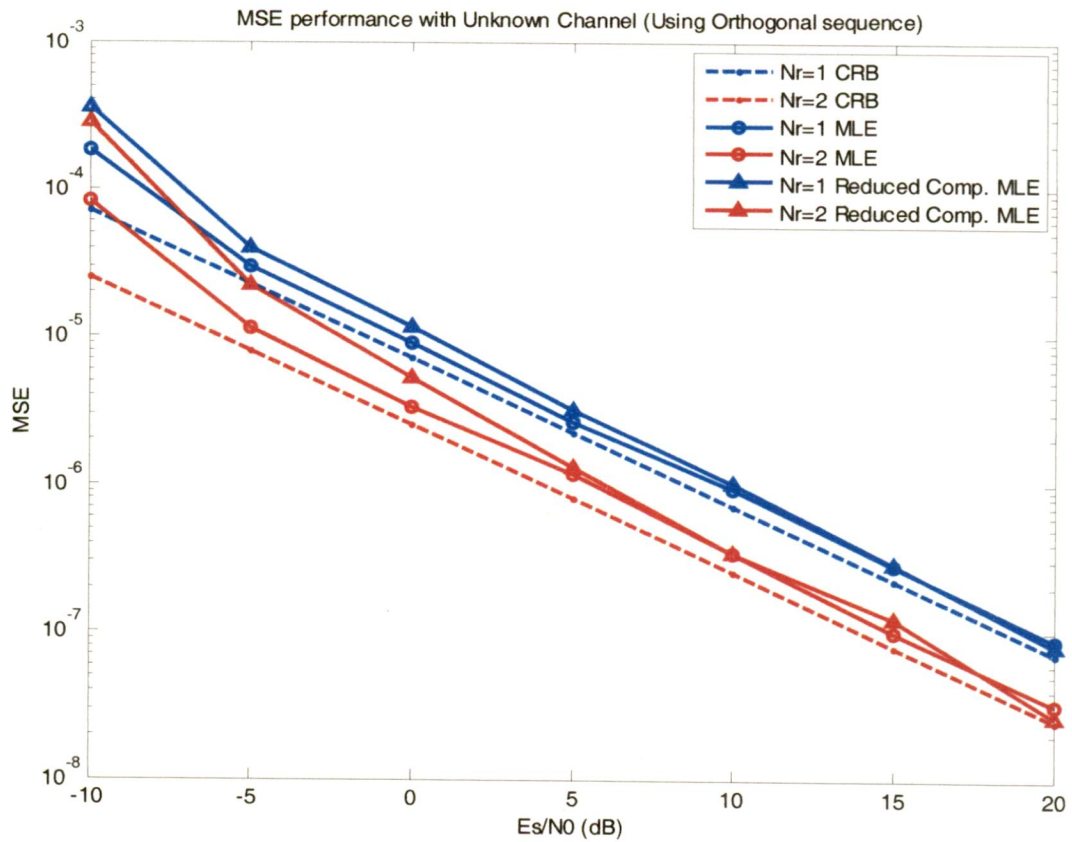


Fig.3.11 Comparison of MSE performance of MLE method and Reduced complexity MLE method simulated for 4 x 1 and 4 x 2 MIMO system (using Orthogonal sequence as training sequence and when channel is Unknown)

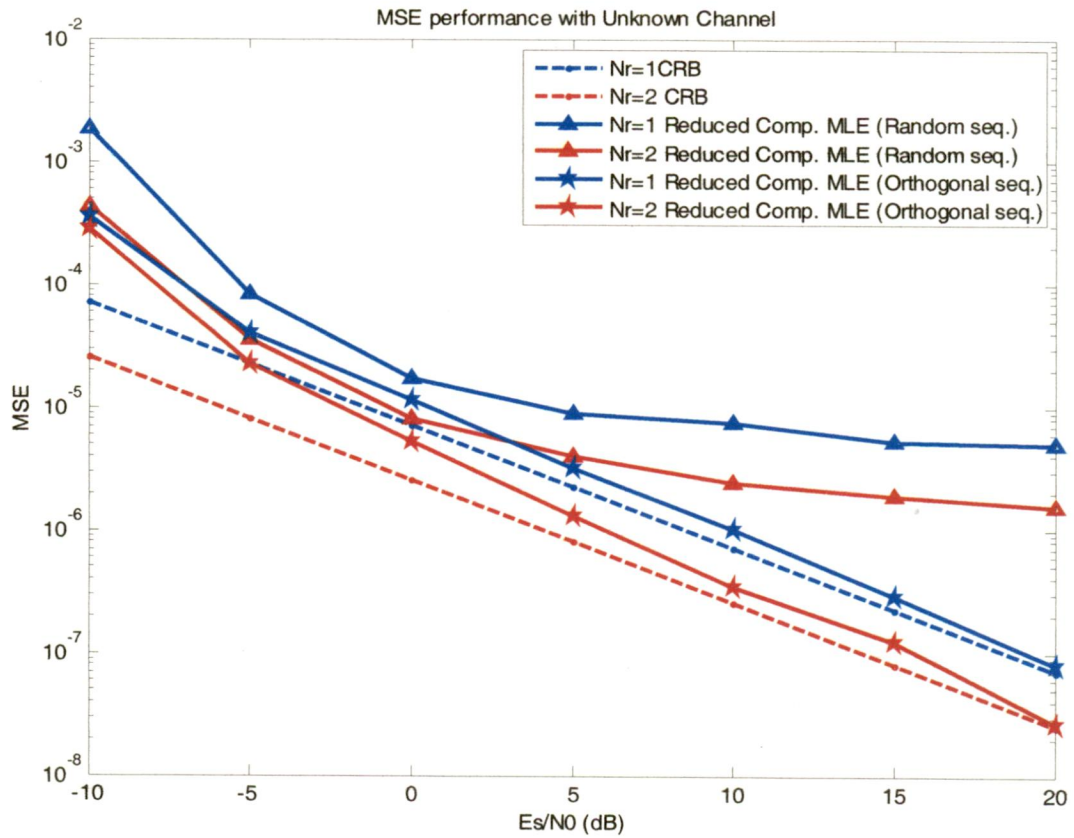


Fig.3.12 Comparison of MSE performance of Reduced complexity MLE method simulated for 4 x 1 and 4 x 2 MIMO system (using both pseudo random sequence and Orthogonal sequence as training sequences and when channel is Unknown)

Chapter-4

Carrier Frequency Offset Estimation in MIMO OFDM Systems

4.1 Introduction

As we know that OFDM is a popular method for high data rate wireless transmission. OFDM may be combined with antenna arrays at the transmitter and receiver to increase the diversity gain and/or to enhance the system capacity on time variant and frequency selective channels, resulting in a multiple-input multiple-output configuration. This combination MIMO OFDM is very beneficial as OFDM will transform each frequency selective MIMO channel into a set of parallel frequency flat MIMO channels and therefore decreases equalization complexity drastically in MIMO systems.

Synchronization is an essential and most important task for any digital communication system. Without a proper accurate synchronization method, it is not possible to reliably receive the transmitted data. It the same case for MIMO OFDM systems too. Failing to synchronize the carrier frequency will destroy the orthogonality between subcarriers and cause ICI. So, accurate estimation and compensation of CFO is very important. But, while considering MIMO OFDM systems there exists multi-antenna interference (MAI) between the received signals from different transmit antennas. The MAI makes CFO estimation more difficult, and a careful training sequence design is required for training-based CFO estimation in case of MIMO systems.

In this section, firstly we will have a brief discussion on Chu sequences. Then after we will have a detailed discussion on CFO estimators for MIMO OFDM systems, which use sequences constructed from Chu sequences as their training sequence. And finally simulation results of the estimators discussed will be produced and compared.

4.2 Chu Sequences

In this section we will have a brief overview on Chu sequences named after its inventor David C. Chu [27]. Polyphase codes with a periodic autocorrelation function, that is zero everywhere except at a single maximum per period have been described by Frank and Zadoff [28] and Heimiller [29]. The lengths of such codes are restricted to perfect squares. But, Chu sequences are the codes with the same correlation properties and can be constructed for any code length.

Consider a code $\{s_k\}$ of length N composed of unity modulus complex numbers, i.e.,

$$s_k = \exp(j\alpha_k) \quad k = 0, 1, \dots, N-1 \quad (4.1)$$

Let autocorrelation function of code sequence $\{s_k\}$ be denoted by $\{x_j\}$. Then it is defined as follows:

$$x_0 = \sum_{k=0}^{N-1} s_k s_k^* \quad (4.2)$$

$$x_j = \sum_{k=0}^{N-j-1} s_k s_{k+j}^* + \sum_{k=N-j}^{N-1} s_k s_{k+j-N}^* \quad j = 1, 2, \dots, N-1$$

It can be shown that for any sequence length N , (i.e. N may be even or odd) the phases α_k can be chosen such that for $j=1, 2, \dots, N-1$, $x_j = 0$ when $j \neq 0$ and x_j will be maximum when $j=0$. If we choose phases $\alpha_k = M\pi k^2/N$ where M is an integer relatively prime to N (and N can be even or odd) then we can get periodic autocorrelation function as mentioned above.

The Real and Imaginary parts of the Chu sequence $\{s_k\}$ with sequence length $N=64$ and $M=21$ are shown in Fig.4.1 (a) and Fig.4.1 (b). Autocorrelation values $\{x_j\}$ are shown in Fig.4.2. Trivial variations such as cyclic shifts, addition of a constant to $\{s_k\}$, or conjugation the entire sequence obviously will not affect the autocorrelation function. In addition, certain linear phase shifts of the form $\exp(j 2\pi qk/N)$, where q is any integer, when introduced into the sequence also will not affect the correlation properties of sequence.

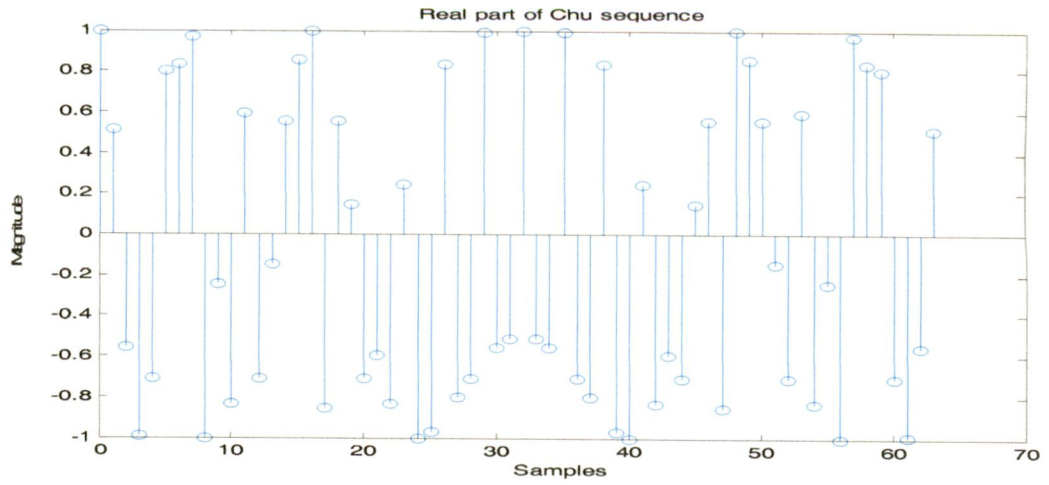


Fig.4.1 (a) Real part of Chu sequence $\{s_k\}$ of length $N=64$ and $M=21$

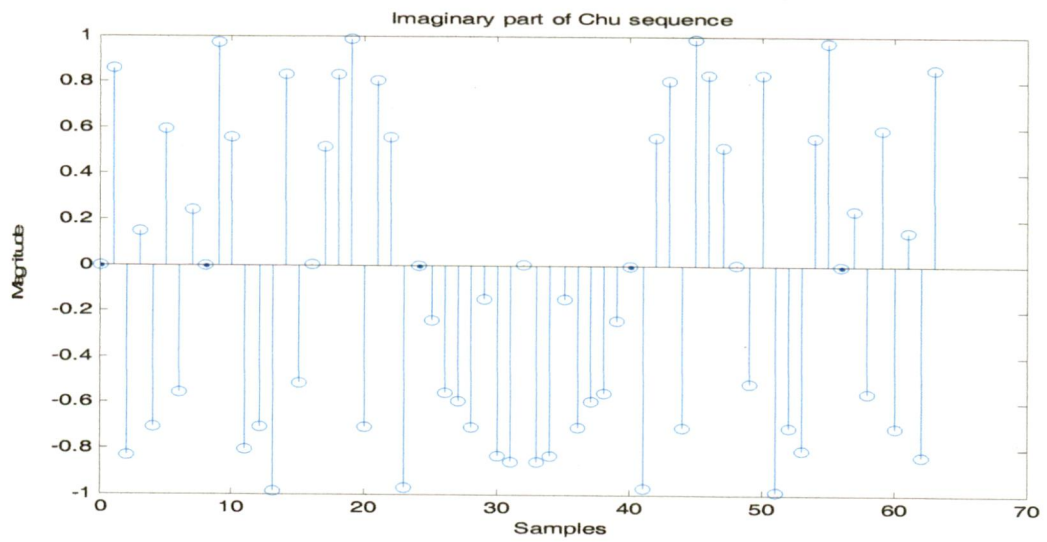


Fig.4.1 (b) Imaginary part of Chu sequence $\{s_k\}$ of length $N=64$ and $M=21$

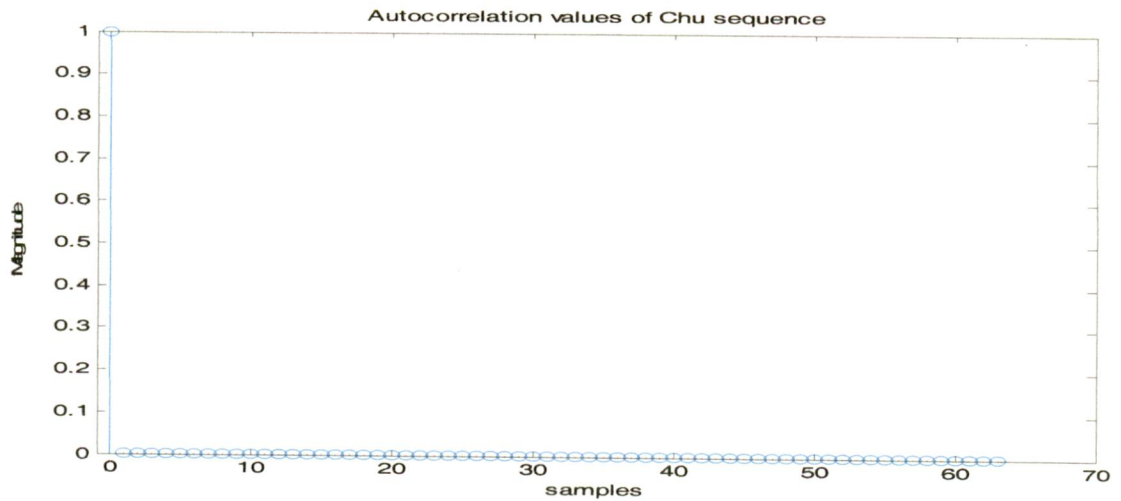


Fig.4.2 Autocorrelation values $\{x_i\}$ of Chu sequence of length $N=64$ and $M=21$

4.3 System Model

Let us consider the MIMO OFDM system with N_T transmit antennas, N_R receive antennas and N subcarriers. Fig.4.3 shows the detailed block diagram of $N_T \times N_R$ MIMO OFDM system. Suppose the training sequence transmitted from the μ^{th} transmit antenna be denoted by $N \times 1$ vector \bar{t}_μ . Before transmission, this vector is processed by an IDFT and a cyclic prefix of length N_g is inserted. Length of N_g is selected such that it is greater than length of the channel L . i.e. $N_g \geq L - 1$. If we assume that all transmit-receive antenna pairs are affected by the same relative CFO ' ε '. Then, the received vector \bar{y}_ν at the ν^{th} receive antenna after removing cyclic prefix of length $N \times 1$ is given by

$$\bar{y}_\nu = \sqrt{N} e^{j2\pi\varepsilon N_g/N} \mathbf{D}_N(\varepsilon) \sum_{\mu=0}^{N_T-1} \left\{ \mathbf{F}_N^H \text{diag} \left\{ \bar{h}^{(\nu,\mu)} \right\} \bar{t}_\mu \right\} + \bar{w}_\nu \quad (4.3)$$

$$\text{where } \mathbf{D}_N(\varepsilon) = \text{diag} \left\{ \left[1, e^{j2\pi\varepsilon/N}, \dots, e^{j2\pi\varepsilon(N-1)/N} \right]^T \right\}$$

\mathbf{F}_N^H is Hermitian of Fast Fourier Transform matrix.

$[\mathbf{F}_N]_{m,n} = \sqrt{N} \exp(-j2\pi mn/N)$ is the $(m,n)^{\text{th}}$ entry of matrix \mathbf{F}_N .

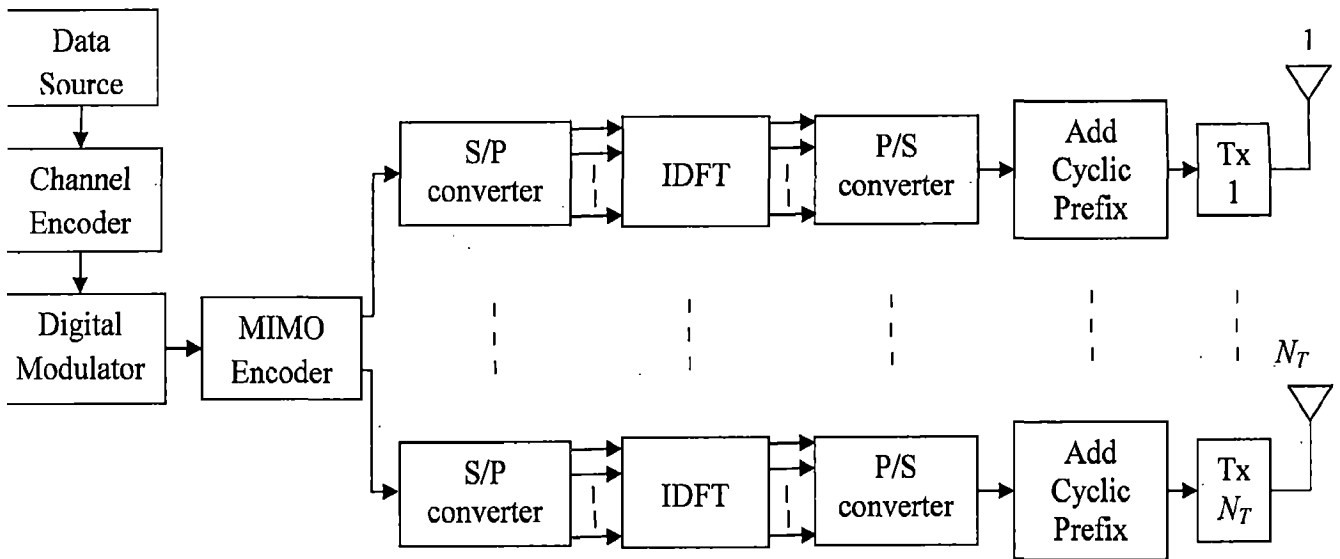
$$\bar{h}^{(\nu,\mu)} = \mathbf{F}_N \left[\bar{e}_N^0, \bar{e}_N^1, \dots, \bar{e}_N^{L-1} \right] \bar{h}^{(\nu,\mu)}$$

$\bar{h}^{(\nu,\mu)}$ is $L \times 1$ vector denoting length- L channel impulse response from the μ^{th} transmit antenna to the ν^{th} receive antenna.

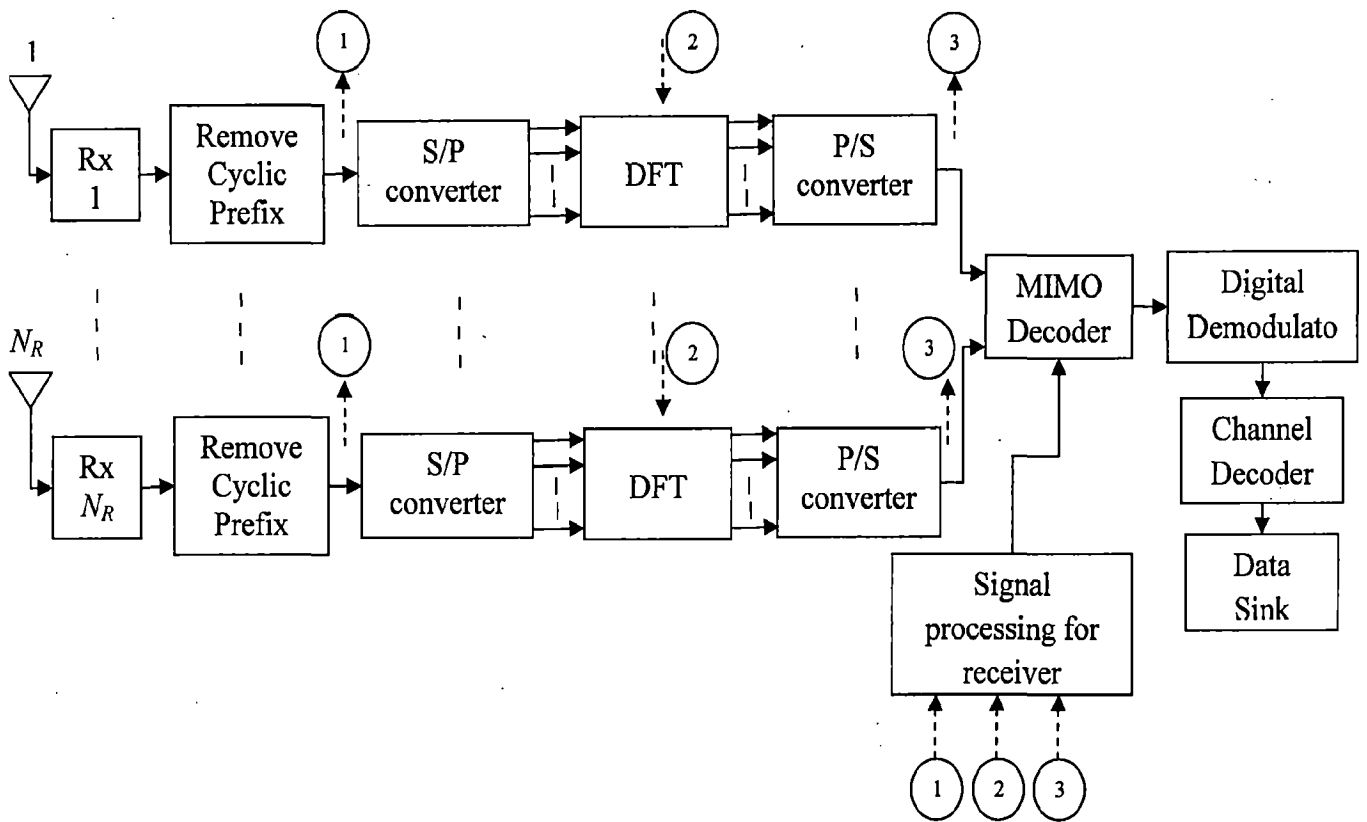
\bar{t}_μ denotes training sequence vector from the μ^{th} antenna of length $N \times 1$

\bar{w}_ν denotes $N \times 1$ vector of additive white complex Gaussian noise with zero mean and σ_w^2 variance.

In the subsequent sections we will use this system model equation (i.e.Eq.(4.3)) for the analysis of the CFO estimators of MIMO OFDM system which use the training sequences that are constructed using Chu sequence.



(a) Transmitter



(b) Receiver

Fig.4.3 Block diagram of $N_T \times N_R$ MIMO OFDM System

4.4 CFO Estimation using Chu sequence based Training sequences (CBTS)

In this section we will discuss one of the effective CFO estimation method for MIMO OFDM system presented by Yanxiang Jiang, Hlaing Minn and Xiqi Gao [30]. This method will estimate the CFO in two parts ; that is integer part known as ICFO and fractional part known as FCFO. This estimation method is a training sequence based estimator and uses the two types of suboptimal training sequences that are constructed using Chu sequence. The constant time domain magnitude of Chu sequence precludes peak-to-average power ratio problems that plague many CP based systems. In addition, certain linear phase shifts when introduced into Chu sequence also will not affect the zero autocorrelation property.

Let \bar{s} denote the Chu sequence of length 'P' and each element of sequence be denoted by

$$[\bar{s}]_p = e^{j\pi L p^2 / P} \quad 0 \leq p \leq P-1 \quad (4.4)$$

where L is co-prime to P

Then, the $P \times 1$ training sequence vector at the μ^{th} transmit antenna is generated from \bar{s}_μ as follows;

$$\bar{s}_\mu = \sqrt{Q/N_T} \mathbf{F}_P \bar{s}^{(\mu M)} \quad (4.5)$$

where $Q = N/P$, $M = \lfloor P/N_I \rfloor$ and $N_I \geq N_T$ are design parameters. \mathbf{F}_P is FFT matrix of size-P.

Let us refer to the training sequence constructed in Eq.(4.5) as Chu sequence based Training sequence 0 (CBTS0) and the training sequence constructed using Eq.(4.6) as Chu sequence based Training sequence 1 (CBTS1).

$$\bar{\tilde{s}}_\mu = \sqrt{Q/N_T} \mathbf{F}_P \bar{s} \quad (4.6)$$

Then, the $N \times 1$ training sequence vector at the μ^{th} transmit antenna is constructed from Eq.(4.5) as follows:

$$\bar{\tilde{t}}_\mu = \Theta_{i_\mu} \bar{\tilde{s}}_\mu$$

where $0 \leq i_\mu \leq Q-1$ and $i_\mu = i_{\mu'}$ iff $\mu = \mu'$.

$$\Theta_q = \left[\bar{e}_N^q, \bar{e}_N^{q+Q}, \dots, \bar{e}_N^{q+(P-1)Q} \right] \text{ and } \bar{e}_N^k \text{ denotes the } k^{\text{th}} \text{ column vector of } \mathbf{I}_N.$$

According to the construction of the training sequences and exploiting the properties of Chu sequence, we note that the proposed training sequences have the following properties [30]:

1. The training sequences are orthogonal to each other
2. All the ‘P’ pilots relevant to each training sequence are uniformly spaced.
3. The time domain sequences corresponding to the proposed frequency domain training sequences have constant amplitude and zero auto-correlation.

For convenience, let us denote $\bar{y} = [\bar{y}_0^T, \bar{y}_1^T, \dots, \bar{y}_v^T, \dots, \bar{y}_{N_R-1}^T]^T$, then this $N_R N \times 1$ cascaded received vector \bar{y} over N_R receive antennas can be written in compact form from Eq.(4.3) as follows.

$$\bar{y} = \sqrt{N} e^{j\frac{2\pi\epsilon N_g}{N}} \left\{ \mathbf{I}_{N_R} \otimes (\mathbf{D}_N(\epsilon) \mathbf{S}) \right\} \bar{h} + \bar{w} \quad (4.7)$$

$$\text{where } \bar{h} = [\bar{h}_0^T, \bar{h}_1^T, \dots, \bar{h}_{N_R-1}^T]^T, \quad \bar{h}_v^T = \left[(h^{(v,0)})^T, (h^{(v,1)})^T, \dots, (h^{(v,N_T-1)})^T \right]^T$$

$$\mathbf{S} = \bar{\mathbf{F}}^H \text{diag} \left\{ [\bar{s}_0^T, \bar{s}_1^T, \dots, \bar{s}_{N_T-1}^T]^T \right\} \check{\mathbf{F}}$$

$$\bar{\mathbf{F}} = \left[\Theta_{i_0}, \Theta_{i_1}, \dots, \Theta_{i_{N_T-1}} \right]^T \mathbf{F}_N$$

$$\check{\mathbf{F}} = \left[\bar{e}_{N_T}^0 \otimes \Theta_{i_0}^T, \bar{e}_{N_T}^1 \otimes \Theta_{i_1}^T, \dots, \bar{e}_{N_T}^{N_T-1} \otimes \Theta_{i_{N_T-1}}^T \right] \left\{ \mathbf{I}_{N_T} \otimes \left[\mathbf{F}_N \left[\mathbf{I}_L, \mathbf{0}_{L \times (N-L)} \right]^T \right] \right\}$$

$$\text{and } \bar{w} = [\bar{w}_0^T, \bar{w}_1^T, \dots, \bar{w}_{N_R-1}^T]^T$$

Taking log-likelihood function of Eq.(4.7) and ignoring the constant terms, we get

$$\ln p(\bar{y}/\epsilon, \bar{h}) = -\sigma_\omega^{-2} \left\| \bar{y} - e^{j\frac{2\pi\epsilon N_g}{N}} \left\{ \mathbf{I}_{N_R} \otimes [\mathbf{D}_N(\epsilon) \mathbf{S}] \right\} \bar{h} \right\|^2 \quad (4.8)$$

Fixing ‘ ϵ ’ and maximizing (Eq.4.8) with respect to \bar{h} , we can get the maximum likelihood (ML) estimate of \bar{h} .

$$\bar{h} = e^{-j\frac{2\pi\epsilon N_g}{N}} \left\{ \mathbf{I}_{N_R} \otimes \left[(\mathbf{S}^H \mathbf{S})^{-1} \mathbf{S}^H \mathbf{D}_N(\epsilon) \right] \right\} \bar{y} \quad (4.9)$$

Substituting the above result back into Eq.(4.9), we can get the ML estimate of ‘ ε ’ by solving the following maximization problem,

$$\tilde{\varepsilon} = \arg \max_{\varepsilon} \left\{ \bar{\mathbf{y}}^H \left[\mathbf{I}_{N_R} \otimes \left[\mathbf{D}_N(\varepsilon) \mathbf{S} (\mathbf{S}^H \mathbf{S})^{-1} \mathbf{S}^H \mathbf{D}_N(-\varepsilon) \right] \right] \bar{\mathbf{y}} \right\} \quad (4.10)$$

$$= \arg \max_{\varepsilon} \left\{ \left\| \mathbf{I}_{N_R} \otimes \left[\mathbf{F}_{N_T P \times N} \mathbf{D}_N(-\varepsilon) \right] \bar{\mathbf{y}} \right\|^2 \right\} \quad (4.11)$$

We notice that matrix inversion is avoided for the ML estimation of ‘ ε ’, which is essentially due to property 1 of the training sequences.

To avoid the large point DFT operation and the time consuming line search and also to guarantee the estimate precision, authors proposed to estimate first integer CFO (ICFO) and then fractional CFO (FCFO). But, the acquisition range of the CFO estimator as shown in Eq.(4.11) with properties will become $(-|Q/2|, |Q/2|)$.

The estimate of ICFO ε_i firstly using N point FFT is given by

$$\tilde{\varepsilon}_i = \arg \max_{\varepsilon_i = (-|Q/2|, |Q/2|)} \left\{ \left\| \mathbf{I}_{N_R} \otimes \left[\mathbf{F}_{N_T P \times N} \mathbf{D}_N(-\varepsilon) \right] \bar{\mathbf{y}} \right\|^2 \right\} \quad (4.12)$$

and ICFO correction could be done by multiplying the received vector $\bar{\mathbf{y}}$ with correction factor $e^{-j \frac{2\pi \tilde{\varepsilon}_i N_g}{N}} (\mathbf{I}_{N_R} \otimes \mathbf{D}_N(-\tilde{\varepsilon}_i))$.

$$\tilde{\bar{\mathbf{y}}} = e^{-j \frac{2\pi \tilde{\varepsilon}_i N_g}{N}} (\mathbf{I}_{N_R} \otimes \mathbf{D}_N(-\tilde{\varepsilon}_i)) \bar{\mathbf{y}} \quad (4.13)$$

The FCFO ε_f should be estimated based on the received vector which is corrected by ICFO correction factor. Assume $\tilde{\varepsilon}_i = \varepsilon_i$ and substitute Eq.(4.7) in Eq.(4.13), then $\tilde{\bar{\mathbf{y}}}$ could be written as follows,

$$\tilde{\bar{\mathbf{y}}} = e^{j \frac{2\pi \varepsilon_f N_g}{N}} \left\{ \mathbf{I}_{N_R} \otimes (\mathbf{D}_N(\varepsilon) \mathbf{S}) \right\} \bar{\mathbf{h}} + \bar{\mathbf{u}} \quad (4.14)$$

$$\text{where } \bar{\mathbf{u}} = e^{-j \frac{2\pi \tilde{\varepsilon}_i N_g}{N}} (\mathbf{I}_{N_R} \otimes \mathbf{D}_N(-\tilde{\varepsilon}_i)) \bar{\mathbf{w}} \quad (4.15)$$

From the properties of the proposed training sequences Eq.(4.14) can be expressed as

$$\bar{\mathbf{y}} = e^{\frac{j2\pi\varepsilon_f N_g}{N}} \left\{ \mathbf{I}_{N_r} \otimes \left[\mathbf{D}_N(\beta_0), \mathbf{D}_N(\beta_1), \dots, \mathbf{D}_N(\beta_{N_T-1}) \right] \bar{\mathbf{S}} \right\} \bar{\mathbf{h}} + \bar{\mathbf{u}} \quad (4.16)$$

$$\text{where } \bar{\mathbf{S}} = \left[\mathbf{I}_{N_r} \otimes \mathbf{1}_Q \otimes \mathbf{f}_P^{0,*}, \dots, \mathbf{I}_{N_r} \otimes \mathbf{1}_Q \otimes \mathbf{f}_P^{P-1,*} \right] \text{diag} \{ \bar{\mathbf{s}} \}$$

From the Eq.(4.16), estimation of the FCFO ε_f is equivalent to estimation of the N_T different equivalent CFO's $\{\beta_\mu\}_{\mu=0}^{N_T-1}$. Using some properties of training sequences and performing algebraic manipulations we can arrive at

$$\mathbf{A} = \mathbf{L}_Q \left[\mathbf{I}_Q - \mathbf{E}_x \mathbf{E}_x^H \right] \mathbf{L}_Q^H \quad (4.17)$$

where \mathbf{L}_Q is the unitary column conjugate symmetric matrix used for transforming the complex covariance matrix into real one.

\mathbf{E}_x is the matrix obtained from the eigen decomposition of the real covariance matrix.

Let us define, $\bar{\alpha}_Q(\beta) = \left[1, e^{j\frac{2\pi\beta}{Q}}, \dots, e^{j\frac{2\pi(Q-1)\beta}{Q}} \right]^T$ then the estimates of $\{\beta_\mu\}_{\mu=0}^{N_T-1}$ correspond to

smallest N_T local minimum of

$$\bar{\alpha}_Q^H(\beta) \mathbf{A} \bar{\alpha}_Q(\beta) \quad (4.18)$$

The local minimum of Eq.(4.18) can be obtained by invoking large point FFT grid searching, but the computational complexity of this approach is very large due to exhaustive search.

In order to compute efficiently, Eq.(4.18) is transformed into a polynomial of degree $2(Q-1)$ using parametric vector $\bar{b}_Q(z) = \left[1, z, \dots, z^{Q-1} \right]^T$ where $z = e^{j\frac{2\pi\beta}{Q}}$. The polynomial is given by

$$f(z) = \bar{b}_Q^T(z) \mathbf{J}_Q \mathbf{A} \bar{b}_Q(z) \quad (4.19)$$

$\{\beta_\mu\}_{\mu=0}^{N_T-1}$ can be indirectly estimated by finding the second order roots of $f(z) = 0$ which are closest to the unit circle. Obtain the final FCFO by averaging $\{\tilde{\epsilon}_{f,n}\}_{n=0}^{2N_T-1}$.

$$\tilde{\epsilon}_f = \frac{1}{2N_T} \sum_{n=0}^{2N_T-1} \tilde{\epsilon}_{f,n} \quad (4.20)$$

we can obtain the whole CFO by simply adding ICFO from Eq.(4.12) and FCFO from Eq.(4.20). i.e.

$$\tilde{\epsilon} = \tilde{\epsilon}_i + \tilde{\epsilon}_f \quad (4.21)$$

Simulation results of this method simulated for 3 X 2 MIMO OFDM system are presented in section 4.5.

4.5 Simplified CFO Estimation using Chu sequence based Training sequence (CBTS)

We know that the maximum Likelihood CFO estimation method is computationally complicated since it requires a large point Discrete Fourier transform operation and time consuming line search. So many reduced complexity algorithms have been proposed in the literature. The one which we have discussed in the section 4.4 is based on the roots directly from the cost function and need the complicated polynomial rooting operation, which is hard to implement in practical OFDM systems.

In this section we will discuss the CFO estimation method which uses a simple polynomial factor method instead of complicated polynomial rooting operation [31]. This method can be implemented via a simple additions and multiplications in practical OFDM system. If we look at the received signal of the MIMO OFDM system Eq.(4.3) and by exploiting the properties of Chu sequences we can write the received vector \bar{y} into the $Q \times N_R P$ matrix \mathbf{Y} .

$$\mathbf{Y} = [\mathbf{Y}_0, \mathbf{Y}_1, \dots, \mathbf{Y}_v, \dots, \mathbf{Y}_{N_r-1}] \quad (4.22)$$

where its elements are given by $[\mathbf{Y}_v]_{q,p} = \left[\left((\bar{e}_{N_r}^v)^T \otimes \mathbf{I}_N \right) \bar{y} \right]_{-qP+p}$

Let us define

$$\bar{\mathbf{b}}_\mu = \left[1, e^{j2\pi(\varepsilon+i_\mu)/Q}, \dots, e^{j2\pi(\varepsilon+i_\mu)q/Q}, \dots, e^{j2\pi(\varepsilon+i_\mu)(Q-1)/Q} \right]^T \quad (4.23)$$

$$\mathbf{B}(\varepsilon) = \left[\bar{\mathbf{b}}_0, \bar{\mathbf{b}}_1, \dots, \bar{\mathbf{b}}_\mu, \dots, \bar{\mathbf{b}}_{N_T-1} \right] \quad (4.24)$$

Then \mathbf{Y} can be expressed in the following equivalent form as

$$\mathbf{Y} = \mathbf{B}(\tilde{\varepsilon})\mathbf{X} + \mathbf{W} \quad (4.25)$$

$$\text{where } \mathbf{X} = \left[\mathbf{X}_0, \mathbf{X}_1, \dots, \mathbf{X}_{N_T-1} \right], \quad \mathbf{X}_v = \left[\bar{x}^{(v,0)}, \bar{x}^{(v,1)}, \dots, \bar{x}^{(v,\mu)}, \dots, \bar{x}^{(v,N_T-1)} \right]^T$$

$$\bar{x}^{(v,\mu)} = \sqrt{P} e^{j2\pi\tilde{\varepsilon}N_s/N} \mathbf{D}_P(\varepsilon + i_\mu) \times \mathbf{F}_P^H \text{diag} \{ \tilde{s}_\mu \} \Theta_{i_\mu}^T \mathbf{F}_N \left[\mathbf{I}_L, \mathbf{0}_{L \times (N-L)} \right]^T \bar{h}^{(v,\mu)}$$

\mathbf{W} is the $Q \times N_T P$ matrix generated from $\bar{\mathbf{w}}$ in the same way as \mathbf{Y} .

According to the multivariate statistical theory, the log likelihood function of \mathbf{Y} conditioned on $\mathbf{B}(\varepsilon)$ and \mathbf{X} can be obtained as follows;

$$\ln p(\mathbf{Y} | \mathbf{B}(\tilde{\varepsilon}), \mathbf{X}) = -\sigma_w^{-2} \text{Tr} \left\{ \left[\mathbf{Y} - \mathbf{B}(\tilde{\varepsilon})\mathbf{X} \right] \left[\mathbf{Y} - \mathbf{B}(\tilde{\varepsilon})\mathbf{X} \right]^H \right\} \quad (4.26)$$

Then after some straight forward manipulations, we obtain the reformulated log likelihood function as follows;

$$\ln p(\mathbf{Y} | \tilde{\varepsilon}) = \text{Tr} \left[\mathbf{B}^H(\tilde{\varepsilon}) \hat{\mathbf{R}}_{\mathbf{Y}\mathbf{Y}} \mathbf{B}(\tilde{\varepsilon}) \right] \quad (4.27)$$

$$\text{where } \hat{\mathbf{R}}_{\mathbf{Y}\mathbf{Y}} = \mathbf{Y}\mathbf{Y}^H$$

Direct grid searching from Eq.(4.27) yields the ML estimate of the carrier frequency offset; however as this method is computationally quite expensive. To efficiently compute the CFO, we will use this simplified CFO estimator for MIMO OFDM systems.

Let $z = e^{j2\pi\varepsilon/Q}$, $z_\mu = e^{j2\pi i_\mu/Q}$ and $\bar{\mathbf{b}}(z) = \left[1, z, \dots, z^q, \dots, z^{Q-1} \right]^T$, then by exploiting the

Hermitian property of $\hat{\mathbf{R}}_{\mathbf{Y}\mathbf{Y}}$, the log-likelihood function in Eq.(4.27) can be transformed into the following equation from

$$f(z) = \bar{\mathbf{c}}^T \left\{ \left[\sum_{\mu=0}^{N_T-1} \bar{\mathbf{b}}(z_\mu) \right] \bar{\mathbf{b}}(z) \right\} + \bar{\mathbf{c}}^H \left\{ \left[\sum_{\mu=0}^{N_T-1} \bar{\mathbf{b}}(z_\mu^{-1}) \right] \bar{\mathbf{b}}(z^{-1}) \right\} \quad (4.28)$$

$$\text{where } \bar{\mathbf{c}} \text{ is a } Q \times 1 \text{ vector with its } q^{\text{th}} \text{ element given by } [\bar{\mathbf{c}}]_q = \sum_{j=i-q} [\hat{\mathbf{R}}_{\mathbf{Y}\mathbf{Y}}]_{i,j} \quad (4.29)$$

From the definition of \bar{c} , we can notice that the q^{th} element of \bar{c} corresponds to the sum of the q^{th} upper diagonal element of $\hat{\mathbf{R}}_{\mathbf{Y}\mathbf{Y}}$. Taking the first order derivate of $f(z)$ with respect to z yields

$$f'(z) = z^{-1} \left\{ \bar{c}^T \left\{ \left[\sum_{\mu=0}^{N_T-1} \bar{b}(z_\mu) \right] \odot \bar{b}(z) \odot \bar{q} \right\} - \bar{c}^H \left\{ \left[\sum_{\mu=0}^{N_T-1} \bar{b}(z_\mu^{-1}) \right] \odot \bar{b}(z^{-1}) \odot \bar{q} \right\} \right\} \quad (4.30)$$

$$\text{where } \bar{q} = [0, 1, \dots, q, \dots, Q-1]^T$$

By letting the derivate of the log-likelihood function $f'(z)$ be zero, the solutions for all local minima or maxima can be obtained. Putting these solutions back into the original log-likelihood function of Eq.(4.28) and select the maximum by comparing all the solutions obtained in the previous stage. Although the search free approach has a relatively lower complexity, it still requires a complicated polynomial rooting operation, which is hard to implement in practical OFDM systems. With the aid of the Chu sequence based training sequence (CBTS) this polynomial rooting operation can be avoided for the training sequence aided CFO estimation in MIMO OFDM system.

If we assume that $P \geq L$, the channel taps remain constant during the training period, and the channel energy is mainly concentrated in the first M taps, with $M < L$. Then, we have

$$c^H \left\{ \left[\sum_{\mu=0}^{N_T-1} b(z_\mu^{-1}) \right] \odot \bar{b}(z^{-1}) \odot \bar{q} \right\} = z^{-Q} k(\iota) \cdot \bar{c}^T \left\{ \left[\sum_{\mu=0}^{N_T-1} \bar{b}(z_\mu) \right] \odot \bar{b}(z) \odot \bar{q} \right\} \quad (4.31)$$

where $k(\iota) = \iota [\bar{c}]_\iota^* / [(\bar{c})_{Q-\iota}]$ with $1 \leq \iota \leq Q-1$, the parameter ι denotes the index of the upper diagonal of $\hat{\mathbf{R}}_{\mathbf{Y}\mathbf{Y}}$.

From Eq.(4.31) we can decompose Eq.(4.30) as follows

$$f'(z) = z^{-(Q+1)} [z^Q - k(\iota)] \cdot \bar{c}^T \left\{ \left[\sum_{\mu=0}^{N_T-1} \bar{b}(z_\mu) \right] \odot \bar{b}(z) \odot \bar{q} \right\} \quad (4.32)$$

Assuming $N_T < Q$ and $\tilde{z} = e^{j2\pi\tilde{\alpha}/Q}$, after some mathematical simplification [5] we get

$$\bar{c}^T \left\{ \left[\sum_{\mu=0}^{N_T-1} \bar{b}(z_\mu) \right] \odot \bar{b}(z) \odot \bar{q} \right\} > 0, \quad f'(\tilde{z}) = 0 \quad (4.33)$$

It follows from Eq.(4.32) and Eq.(4.33) that $z = \bar{z}$ is one of the roots of both $f'(\bar{z}) = 0$ and $z^Q - k(\iota) = 0$. Unlike $f'(\bar{z}) = 0$, the roots of $z^Q - k(\iota) = 0$ can be calculated without the polynomial rooting operation. Therefore by solving the simple polynomial equation $z^Q - k(\iota) = 0$, the CFO estimate can be efficiently obtained as follows;

$$\hat{\varepsilon} = \arg \max_{\varepsilon \in \{\varepsilon_q\}_{q=0}^{Q-1}} \{f(z) | z = e^{j2\pi\varepsilon/Q}\} \quad (4.34)$$

$$\text{where } \varepsilon_q = \arg\{k(\iota)\} / (2\pi) + q - Q/2$$

If we compare the CFO estimation method discussed in section 4.4 with the method discussed in this section, we find that this method is computationally efficient one as polynomial rooting operation is avoided and can be easily implemented via simple additions and multiplications in practical OFDM systems.

4.6 Simulation Results

4.6.1 Simulation Results of method discussed in section 4.4

To perform CFO estimation using Chu sequence based training sequences for MIMO OFDM system as discussed in section 4.4, we use the following parameters;

- Assumption : *All transmit/receive antenna pairs are affected by same CFO*
- No. of Transmit antennas : $N_T = 3$
- No. of Receive antennas : $N_R = 2$
- No. of subcarriers : $N = 1024$
- Guard interval : $N_g = 64$
- Training sequence used : *Random sequence and Chu sequence based training sequences (CBTS0 & CBTS 1)*
- Training sequence parameters : $P = 64$ and $Q = 16$
- Each channel has : *4 independent Rayleigh fading taps whose average powers and propagation delays are $\{0, -9.7, -19.2, -22.8\}$ dB and $\{0, 0.1, 0.2, 0.4\}$ us respectively.*
- Modulation scheme used : *QAM modulation*
- SNR values taken : $\{0, 5, 10, 15, 20\}$ dB
- No. of Monte Carlo simulation trials : 10^6

Fig.4.4 shows the Mean Square Error (MSE) results of the estimation method discussed in section 4.4 using different types of training sequences. We can note from the plot that the performance of estimator using Chu sequence based training sequence is better than random sequence. If we compare CBTS0 and CBTS1 performance, CBTS0 performance is little more better than CBTS1 and approaches CRLB.

4.6.2 Simulation Results of method discussed in section 4.5

To perform CFO estimation using Chu sequence based training sequences for MIMO OFDM system using simplified estimator as discussed in section 4.5, we use the following parameters;

- Assumption : *All transmit/receive antenna pairs are affected by same CFO*
- No. of Transmit antennas : $N_T = 3$
- No. of Receive antennas : $N_R = 2$
- No. of subcarriers : $N = 1024$
- Guard interval : $N_g = 64$
- Training sequence used : *Random sequence and Chu sequence based training Sequence (CBTS1)*
- Training sequence parameters : $P = 64$ and $Q = 16$
- Each channel has : 4 independent Rayleigh *fading taps whose average powers and propagation delays are $\{0, -9.7, -19.2, -22.8\}$ dB and $\{0, 0.1, 0.2, 0.4\}$ us respectively.*
- Modulation scheme used : *QAM modulation*
- SNR values taken : $\{0, 5, 10, 15, 20\}$ dB
- No. of Monte Carlo simulation trials : 10^6

Fig.4.5 shows the Mean Square Error (MSE) results of the simplified estimation method used for MIMO OFDM system that is discussed in section 4.5 using different types of training sequences. We can note from the plot that the performance of estimator using Chu sequence based training sequence is better than random sequence.

Fig.4.6 shows the MSE performance of the both estimation methods i.e. polynomial rooting method (discussed in section 4.4) and computationally simplified estimation method (discussed in section 4.5) using CBTS. We can see that the performance of computationally simplified estimation method is close to the one which is discussed in section 4.4.

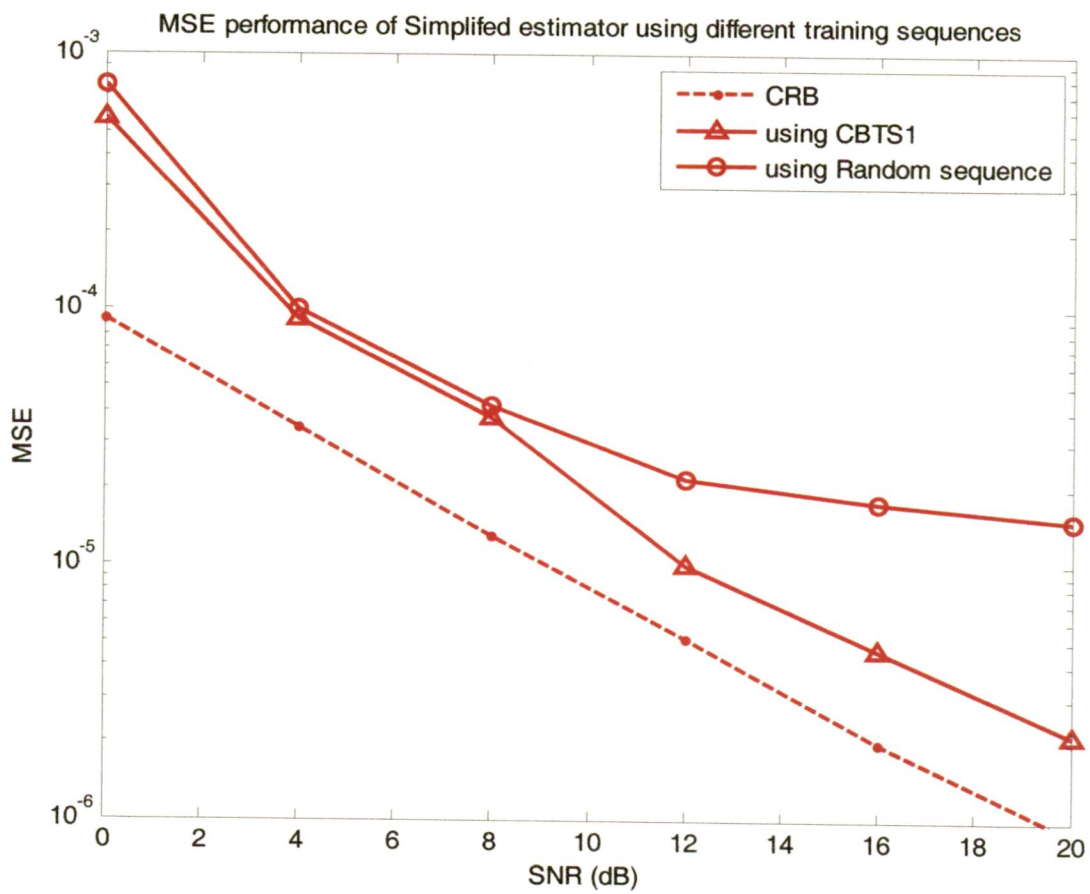


Fig.4.5 MSE performance of 3 x 2 MIMO OFDM system with simplified estimator using different training sequences

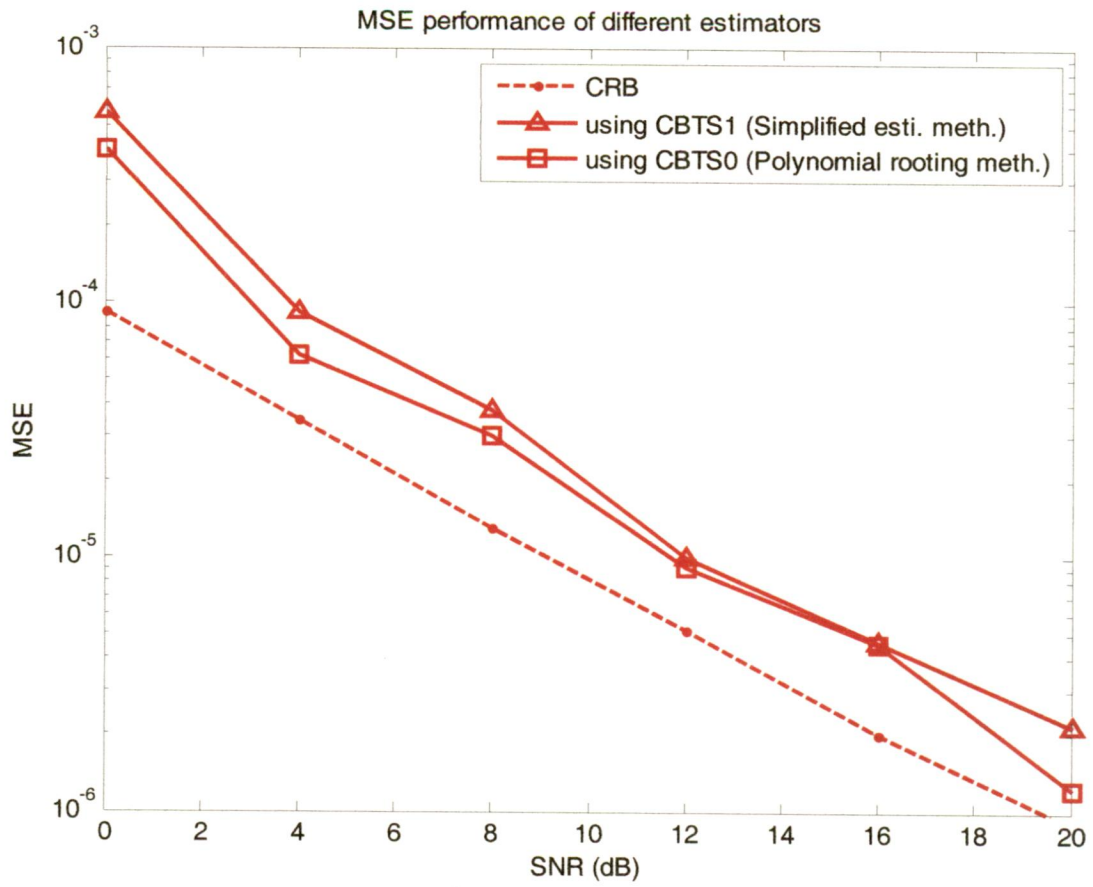


Fig.4.6 MSE performance of 3 X 2 MIMO OFDM system using different estimators using Chu sequence based training sequences (CBTS)

Chapter-5

Conclusions

The basic and most essential task that is to be performed in any digital communication system is synchronization, without which a reliable reception of transmitted data is quite impossible. Synchronization for any digital communication system can be viewed in two parts: *Carrier frequency synchronization* and *Symbol timing synchronization*. Carrier frequency synchronization or estimation can be performed in two ways: *Training sequence based estimation* and *Blind estimation*. Even though training sequence based estimation methods are slightly spectral inefficient than blind ones, their computational complexity is less. So, they are the mostly used ones in practical systems.

This dissertation work is aimed at performance study of training sequence based Carrier Frequency Offset (CFO) estimation methods that are used for MIMO and MIMO OFDM systems. The conclusions that are drawn from the previous discussions and simulation results are as follows

CFO Estimation in MIMO Systems

- We have investigated above computationally intensive Maximum Likelihood (ML) estimation method and from their simulation results we observed that it will give optimal estimation values even using pseudo random sequence as training sequence. From its MSE performance results we observe that at higher SNR values its performance attains the Cramer-Rao Lower Bound (CRLB), which is the benchmark, showing the lowest value that cannot be crossed by any unbiased estimator.
- We have also looked at computationally efficient ML estimation method and observed that this method will not attain the optimum performance even at higher SNR values due to the presence of noise floor created by training sequences transmitted from other transmit antennas at the same time. In order to remove this noise floor orthogonal training sequence is used. From simulation results obtained using this orthogonal training

sequences, we can observe that MSE performance of computationally efficient ML estimation method approaches the performance of ML estimation method at higher values of SNR.

CFO Estimation in MIMO OFDM System

- We have investigated CFO estimator for MIMO OFDM systems, which use zero auto correlation propertied Chu sequence based training sequences (CBTS) for estimation purpose. It estimates CFO using polynomial rooting technique, which is computationally complex and hard to implement in practical OFDM system. From simulation results we can observe that MSE performance of this method approach CRLB for higher values of SNR. We can also observe that even for pseudo random sequence the MSE performance is attaining the acceptable level.
- We have also looked at another CFO estimator which also uses CBTS and factor decomposition method for finding the estimate value, whose computational complexity is much lesser than the earlier method. From simulation results we observe that the MSE performance approaches CRLB for higher SNR values. But same is not true when pseudo random sequence is used as training sequence.
- If we observe the MSE performance of both methods we can see that the performance of computationally efficient estimation method using CBTS is quite similar to computationally intensive method.

Scope of Future Work

- As we know, along with the accuracy of the estimate consistency is also an important parameter to be considered for any estimator. Its importance can be observed when the communication link is emergency and crucial. So robust and consistent training sequence design for carrier frequency offset estimation in MIMO and MIMO OFDM systems can be a possible line of future work.

REFERENCES

- [1] Theodore S. Rappaport, "Wireless Communications - Principles and Practice," 2nd Edition, Prentice Hall, 2000.
- [2] Shinsuke Hara and Ramjee Prasad, "Multicarrier Techniques for 4G Mobile Communications," Artech House, 2002.
- [3] R.W.Chang and R.A. Gibbey, "A Theoretical Study on Performance of an Orthogonal Multiplexing Data Transmission Scheme," IEEE Transaction on Communication, vol. 16, no. 4, pp. 529-540, June 1968.
- [4] P.Warrier and B. Kumar, "xDSL Architecture," McGraw Hill, 2000.
- [5] IEEE standards for Information Technology – Telecommunications and Information Exchange between Systems – Local and Metropolitan Area Networks – Specific requirements – Part 11: Wireless LAN Medium Access Control (MAC) and Physical Layer (PHY) specifications – Amendment 1: High-Speed Physical Layer in the 5 GHz band, 802-11: 1999, 2000.
- [6] IEEE standards for Information Technology – Telecommunications and Information Exchange between Systems – Local and Metropolitan Area Networks – Specific requirements – Part 11: Wireless LAN Medium Access Control (MAC) and Physical Layer (PHY) specifications – Amendment 4: Further Higher-Speed Physical Layer Extension in the 2.4 GHz band, IEEE 802.11g: 2003, 2003.
- [7] J.Lorincz and D.Begusic, "Physical Layer Analysis of Emerging IEEE 802.11n WLAN Standard," in IEEE Proceedings ICACT'2006, vol. 1, no. 4, pp. 383-387, Feb. 2006.
- [8] J.Z.Sun, et al., "Features in Future: 4G Visions from a Technical Perspective," in IEEE Proceedings GLOBECOM'2001, vol. 6, no.4, pp. 3533-3537, Nov. 2001.
- [9] T.Pollet, M.Van Bladel and M.Moeneclay, "BER Sensitivity of OFDM Systems to Carrier Frequency Offset and Wiener Phase Noise," IEEE Transaction on Communication, vol. 43, no. 2, pp.191-193, Feb. 1995.

- [10] G. L. Stuber, J. R. Barry, S. Mclaughlin, Y. Li, M. A. Ingram, and T. G. Pratt, "Broadband MIMO OFDM Wireless Communications," in *IEEE Proceedings*, vol. 92, no. 2, pp. 271–294, Feb. 2004.
- [11] T.M. Schmidl and D.C. Cox, "Robust Frequency and Timing Synchronization for OFDM," *IEEE Transaction on Communication*, vol. 45, no. 12, pp. 1613–1621, Dec. 1997.
- [12] H. Nagami and T. Nagashima, "A Frequency and Timing Period Acquisition Technique for OFDM Systems," in *IEEE Proceedings PIMRC'95*, vol. 3, pp. 1010–1015, Sep. 1995.
- [13] J.J. van de Beek, M. Sandell and P.O. Borjesson, "ML Estimation of Time and Frequency Offset in OFDM Systems," *IEEE Transaction on Signal Processing*, vol. 45, no. 7, pp. 1800–1805, July 1997.
- [14] F. Daffara and A. Chouly, "Maximum Likelihood Frequency Detectors for Orthogonal Multi-Carrier Systems," in *IEEE Proceedings ICC'93*, vol. 2, pp. 766–771, May 1993.
- [15] U. Tureli and H. Liu, "Blind Carrier Synchronization and Channel Identification for OFDM Communications," in *IEEE Proceedings ICASSP'98*, vol.6, pp. 3509–3512, May 1998.
- [16] Y. Yao and G. B. Giannakis, "Blind Carrier Frequency Offset Estimation in SISO, MIMO and Multiuser OFDM Systems," *IEEE Transaction on Communication*, vol. 53, no. 1, pp. 173–183, Jan. 2005.
- [17] P. Moose, "A Technique for Orthogonal Frequency Division Multiplexing Frequency Offset Correction," *IEEE Transaction on Communication*, vol. 42, no.10, pp. 2908– 2914, Oct. 1994.
- [18] G. J. Foschini and M. J. Gans, "On Limits of Wireless Communication in a Fading Environment when using Multiple Antennas," *IEEE Transaction on Wireless Communication*, vol. 6, no. 3, pp. 311–335, Mar. 1998.
- [19] D. C. Rife and R. R. Boorstyn, "Single Tone Parameter Estimation from Discrete-Time Observations," *IEEE Transaction on Information Theory*, vol. 20, no. 5, pp. 591–598, Sep. 1974.
- [20] M. Luise and R. Reggiannini, "Carrier Frequency Recovery in All-Digital Modems for Burst-mode Transmissions," *IEEE Transaction on Communication*, vol. 43, no. 2/3/4, pp. 1169–1178, Feb./Mar./Apr. 1995.

- [21] M. P. Fitz, "Further Results in the Fast Estimation of a Single Frequency," *IEEE Transaction on Communication*, vol. 42, no. 2, pp. 862–864, Feb. 1994.
- [22] F. Simoens and M. Moeneclaey, "Reduced Complexity Data-Aided and Code-Aided Frequency Offset Estimation for Flat-Fading MIMO Channels," *IEEE Transaction on Wireless Communication*, vol. 5, no. 6, pp. 1558–1567, June 2006.
- [23] D. K. Hong, Y. J. Lee, D. Hong, and C. E. Kang, "Robust Frequency Offset Estimation for Pilot Assisted Packet CDMA with MIMO Antenna Systems," *IEEE Transaction on Communication*, vol. 6, no. 6, pp. 262–264, June 2002.
- [24] F. Simoens and M. Moeneclaey, "A Reduced Complexity Frequency Offset Estimation Technique for Flat-fading MIMO Channels," in *IEEE Proceedings CASSET'2004*, vol.3, pp. 705–708, 2004.
- 25] T. L. Marzetta, "BLAST Training: Estimating Channel Characteristics for High Capacity Space-Time Wireless," in *IEEE Proceedings AAC'1999*, vol. 2, pp. 958–966, Sep. 1999.
- 26] Cramer Harald, "Mathematical Methods of Statistics," Princeton university press, 1946.
- 27] David C. Chu, "Polyphase Codes with Good Periodic Correlation Properties," *IEEE Transaction on Information Theory*, vol. 18, pp. 531-532, July 1972.
- 28] R. L. Frank and S. A. Zadoff, "Phase Shift Pulse Codes with Good Periodic Correlation Properties," *IRE Transaction on Information Theory*, vol. IT-8, pp. 381-382, Oct. 1962.
- 29] R. C. Heimdlar, "Phase Shift Codes with Good Periodic Correlation Properties," *IRE Transaction on Information Theory*, vol. IT-7, pp. 254-257, Oct. 1961.
- 30] Y. Jiang, H. Minn, X. Gao, X. You, and Y. Li, "Frequency Offset Estimation and Training Sequence Design for MIMO OFDM," *IEEE Transaction on Wireless Communication*, vol. 7, no. 4, pp. 1244–1254, Apr. 2008.
- 31] Y. Jiang, H. Minn, X. You and X. Gao, "Simplified Frequency Offset Estimation for MIMO OFDM Systems," *IEEE Transaction on Vehicular Technology*, vol. 57, no. 5, pp. 3246-3251, Sep. 2008.